NORTHWESTERN UNIVERSITY

# Elucidating biofilm pH dynamics in minimally buffered environments

A DISSERTATION

SUBMITTED TO THE GRADUATE SCHOOL

IN PARTIAL FULFILLMENT OF THE REQUIREMENTS

for the degree

DOCTOR OF PHILOSOPHY

Field of Chemical and Biological Engineering

By

Peter Tran

EVANSTON, ILLINOIS

September 2023

# ABSTRACT

Elucidating biofilm pH dynamics in minimally buffered environments

Peter Tran

Bacteria represent the most abundant form of life on Earth and have evolved to successfully colonize nearly every environmental niche. In doing so, bacteria predominately form multicellular communities known as biofilms, resulting in increased resilience, persistence, and emergent behaviors. Consequently, biofilms present an attractive target for engineering and synthetic biology, as understanding biofilm physiology can elucidate mechanisms enabling pathogenic biofilms and provide new modalities for multicellular control. While biofilms provide individual bacteria many advantages, the dense cellular proliferation can also create intrinsic metabolic challenges including excessive acidification. Because such pH stress is commonly masked in buffered laboratory media, it remains unclear how biofilms cope with minimally buffered natural environments. In this work, we develop several methods to interrogate biofilm physiology, metabolism, and underlying pH dynamics under minimally buffered conditions.

This dissertation details methods for studying biofilm pH dynamics. In doing so, we establish a toolbox which enables observation of a previously unseen pH dynamic. The

primary efforts towards that are 1) using metabolic flux analysis to study biofilm energy metabolism *in situ* and 2) employing a suite of genetic screens, -omics, and microscopy to elucidate biofilm pH dynamics. We report *Bacillus subtilis* biofilms overcome this intrinsic metabolic challenge through an active pH regulation mechanism. Specifically, we find that biofilms can modulate their extracellular pH to the preferred neutrophile range, even when starting from acidic and alkaline initial conditions, while planktonic cells cannot. We associate this behavior with dynamic interplay between acetate and acetoin biosynthesis and show that this mechanism is required to buffer against biofilm acidification. Furthermore, we find that buffering-deficient biofilms exhibit dysregulated biofilm development and increased sensitivity to antibiotics when grown in minimally buffered conditions.

This dissertation elucidates an emergent pH regulation behavior in biofilms that enable them to develop and persist that in future work could be targeted to control and engineer biofilm growth.

## Acknowledgements

The PhD journey is often described as a marathon, running for what feels like an eternity and wondering if the finish line will ever appear. Over these past 7 years, I was blessed to learn that this race is not at all impossible, thanks to the kind support of mentors, friends and family.

To my advisor, Dr. Arthur Prindle, thank you for your mentorship and making the most welcoming lab environment. I am truly grateful for our countless meandering conversations about science, philosophy, and wacky conspiracy topics.

To my PhD committee, Dr. Keith Tyo, Dr. Danielle Tullman-Ercek, and Dr. Julius Lucks, thank you for you support and guidance during my PhD. All of you have shown me what it means to be exemplary scientists, teachers, and communicators.

To my former supervisors, Dr. Upma Sharma and Dr. Dan Bonner, thank you for inspiring me to aim higher.

To my fellow cohort members, grad school would have been much less joyful without you all. The normal troughs of PhD life were offset by the hysterical laughing during statistical mechanics exams, trivia, and potlucks. To Andrew and Alex, thank you for being amazing housemates/cookie dough consumers. To Adam, thank you for your incredible trivia knowledge. To Kevin, thank you for being my roommate during our recruitment visit and being a great sanity check as we both transferred labs. To Jon, thank you for

being my lifting/catsitting/board game buddy. To Jake and Erika, thank you for all the Gloomhaven shenanigans and snacks.

To my lab mates, Stephen, Corey, Garth, Blake, Sarah, Jon, and Keren, thank you for being wonderful friends that make coming to lab all the better. You all inspire me to be a better scientist and connoisseur for finding free food.

To my friends, you provided a precious outlet outside of science that truly kept me sane. To Callen, thank you for this shockingly old friendship and all the Jack Burton quotes. Yessir, the check is in the mail. To Thayer, thank you for being the goodest boy. To Melanie, thank you for being amazing and sending the most curated memes. To Sheetal, thank you for being so bright and goofy, and sending that diabolical game of the Fuzzies. To Kassi, thank you for always being down to vent about science. To Sophia, thank you for always listening and being so thoughtful. Your emotional intelligence and style enrich my days. To Yue and Karl, thank you for always ordering too much food and being incredible hosts. It was an honor to be part of your wedding. To Nicole, thank you for sharing all your stories and exquisite tastes. To Josh, thank you for being an excellent dance/cycling/wine friend. I deeply enjoy how we can geek out about anything. To Michael, thank you for sharing your love of board games. To Jerome, thank you for being so copacetic.

To my family, Mom, Ba, and Rebecca, thank you for supporting me no questions asked. Not technically the doctor you had hoped for, but I still get to wear a fancy robe. All the care packages meant the world to me (including the frozen meats in my carry-on).

To Lila, thank you for being the loveliest little spectre. You have provided great joy and comfort during this journey with your silent observation, mandatory keyboard inspections, and targeted sternum stomps.

Finally to Angelia, thank you for being the most wonderful partner. You have lifted me up on my lowest days and have been the highlight of my best days. It is truly a blessing to have a co-conspirator who will go to grocery stores just for fun, dance at Carly Rae Jepsen concerts, do the crossword in bed, and go on long walks as verified by Strava. This journey would have been impossible without you.

# Table of Contents

# List of Figures

CHAPTER 1

# Introduction

Bacteria inhabit a diverse range of environmental niches and engage in specific lifestyles to thrive within their local environment. In controlled laboratory conditions, bacteria primarily exist as planktonic (free-swimming) individuals whereas in natural environments bacteria often form sessile, multicellular communities known as biofilms [**1, 2**]. Biofilms create a densely packed local environment with extracellular matrix (ECM) [**3, 4**] that can give rise to complex emergent behaviors such as cell-to-cell signaling [**5, 6**], macroscopic spatiotemporal organization [**7, 8, 9**], and metabolic remodeling [**10, 11**]. Furthermore, the biofilm structure creates a diffusion barrier and resulting local concentration gradients, producing habitat diversity and increased resilience against antibiotics [**12, 13, 14**]. Thus, the biofilm state confers advantages to individual bacteria unavailable to planktonic cells.

These advantages enable biofilms to be distinctly resilient and persistent in environments, which make biofilms attractive targets for medicine and engineering. While common methods of studying microorganisms have been practiced for decades and have been instrumental to fundamental discoveries in pathogenesis and microbial physiology, these microbiology techniques are often not readily applied to biofilms due to their architectural and compositional complexity [**15, 16**]. Biofilms are physiologically distinct from their planktonic counterparts and therefore require new methods to decipher their unique physiology. By developing tools to expand the field of microbiology towards the natural biofilm context, we will increase our understanding of the biology behind infection,

ecological processes, bioreactor design, and other processes mediated by microorganisms [**17, 1, 18, 19**]. Furthermore, by gaining such insights into biofilm physiology, we will reveal new strategies for more effective antibiotic treatment in the context of disease and enable engineering bacteria in new modalities.

This introduction section will cover synthetic biology in biofilms, with focus on 1) recent advances in tools for engineering biofilms, 2) remaining challenges, and 3) opportunities for increased understanding of biofilm physiology and engineered biofilms.

### 1.1. Synthetic biology in biofilms

Bacteria are readily modifiable chassis organisms with diverse biochemical repositories of genes and proteins that could be leveraged for synthetic biology. However, much of bacterial synthetic biology remains focused on a handful of domesticated and planktonic bacterial species that have been optimized for the laboratory [**20**]. As a result, deploying these engineered bacteria into key target environments remains challenging since these cells experience heterogeneous conditions that result in non-optimal performance and an inability to persist in the environment [**21**]. Bacteria in natural environments predominately reside in the context of densely packed multicellular communities known as biofilms [**1**]. Biofilms account for nearly 80% of all bacteria on the planet, occupying environments that span from miles underneath the ocean floor to inside of the human gastrointestinal tract [**2**]. Bacteria within biofilms can undergo significant shifts in gene expression and participate in emergent social behaviors including division of labor and coordinated growth [**22, 23, 24**]. These processes enable collective organization and the formation of macroscopic structures that enable more efficient distribution of resources

and mechanical resilience [**3, 25**]. Furthermore, these bacteria facilitate population-level coordination though cell-to-cell signaling such quorum sensing and ion channel-mediated communication [**24, 5, 26**].

Due to their prevalence in nature and innate emergent properties, biofilms present synthetic biology the attractive opportunity to deliver and operate engineered gene circuits in a range of desired target environments, such as soil and the microbiome. More generally, collective organization has been a long-coveted goal for the field of synthetic biology and tapping into the native capabilities found in biofilms may enable the next generation of spatiotemporally controlled gene circuit designs. This review provides a brief overview of recent developments toward synthetic biology in biofilms, with focuses on molecular tools, biological challenges, and potential opportunities for engineered biofilms (Figure 1.1).

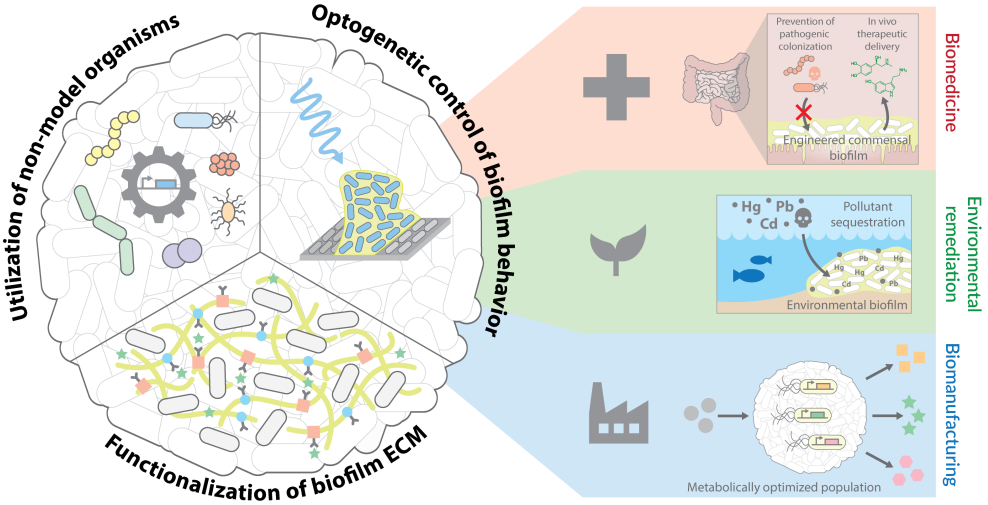


**Figure 1.1.** Recent tools and potential applications for synthetic biology in bacterial biofilms

### 1.1.1. Tools for synthetic biology in biofilms

Inspired by the biology of natural microbial communities and biofilms, synthetic biology is shifting from engineering single cells and model species to engineering microbial consortia that may be composed of multiple species [**27, 28, 29, 30, 31**]. To realize this shift, the field will need to create new tools that 1) Expand the synthetic biology tool set towards non-model and undomesticated bacterial species; 2) Harness optogenetics to control and coordinate larger diffusion-limited cellular populations; and 3) Functionalize the biofilm extracellular matrix to control the spatial and temporal arrangement of bacteria within the consortia. These tools will further enable the effective deployment of engineered bacteria into natural target environments by harnessing the unique physiology of biofilms.

**1.1.1.1. Expansion of genetic tools towards non-model biofilm species.** While domesticated bacterial strains can be used to prototype new synthetic designs in the lab, deploying these cells into nature remains a challenge as they experience heterogeneous environmental conditions that can impact cellular fitness [**21**]. To address this shortcoming, recent efforts have focused on expanding the synthetic biology toolbox towards new bacterial species beyond *Escherichia coli* (*E. coli*). A foundational set of characterized promoters, ribozyme binding sites, and protein degradation tags was created for biofilm-forming *Bacillus subtilis* (*B. subtilis*) [**32**]. This was further expanded to include more inducible promoters and integration vectors for delivering DNA into the *B. subtilis* chromosome at specific sites such as the sacA and amyE loci [**33**]. The RSF1010 replicon was used to create a parts library that can be used to assemble broad-host-range plasmids in species of *Proteobacteria* that commonly colonize the bee gut [**34**].

While the number of genetic parts for synthetic circuits is increasing, these parts continue to be created on a per-species basis. For engineering multi-species communities such as microbiomes in the soil or mammalian gut, there remains a need to broadly transform microbial systems in place using native microbial consortia. To address this need, bacterial conjugation has recently been leveraged to efficiently deliver DNA into undomesticated bacteria across a broad spectrum of species. During conjugation, a host cell attaches a pilus to a recipient allowing the direct cell-to-cell transfer of DNA and homologous recombination integrates this DNA into the recipient genome [**35**]. Engineered E. coli was able to deliver biosynthetic gene clusters into the chromosomes of bacteria species across multiple phyla, using conjugation to transfer DNA, a transposon system to integrate a landing pad into the recipient chromosome, and Lac-T7 expression system to tightly control expression of BGCs in the recipient [**36**]. The IncP$\alpha$-family RP4 conjugation system enabled an *E. coli* donor strain to transfer a synthetic cassette into both Gram-negative and positive microbiota species in a mouse gastrointestinal tract [**37**]. Integrative and conjugative elements *B. subtilis* were engineered as to allow delivery synthetically designed DNA into the chromosomes of the recipient even under non-ideal conditions such as in the soil [**38**].

The field of synthetic biology has begun to utilize non-model and undomesticated bacterial species though the creation of new genetic parts and broad range genetic transformation methods. Future challenges will include maintenance and containment of these engineered functions in their native contexts, such as soil and the microbiome.

**1.1.1.2. Optogenetic control over bacterial biofilm behavior.** Most synthetic biology designs utilize small molecule inducers which require sufficient concentration in

the environment as well as homogeneous diffusion throughout the cellular community. These requirements can be difficult to achieve in conditions of non-ideal environmental mixing and dense cellular growth, such as found in biofilms. As a result, the field is moving to leverage optogenetics, where exposure to specific wavelengths of light trigger gene expression on demand in a defined manner. Such an approach would allow control of engineered cells even in complex natural environments where it is not practical to achieve high and uniform inducer concentrations. Considering these challenges, Optogenetic approaches may provide dynamic control of spatiotemporal induction that could not be achieved with a small molecule inducer alone. With precise spatiotemporal light exposure across multiple wavelengths, biofilm cells can be patterned to aggregate in specific patterns with micron precision. Photoreceptors and their associated transcriptional regulators from plants and cyanobacteria have been leveraged to create light-responsive elements that regulate expression of biofilm matrix components and subsequently biofilm structure. Blue light was used to activate the transcriptional promoter pDawn and adhesion gene Ag43 expression, enabling lithography of *E. coli* biofilms [**39**]. Blue light exposure was also shown to persistently and robustly change the membrane potential dynamics in a *B. subtilis* biofilm, with the effect remaining for hours after the initial stimulus suggesting a form of cellular memory [**40**]. Near-infrared (NIR) was used to control target gene expression in *E. coli* via NIR-responsive photoreceptor BphP1 and its interacting transcriptional repressor PpsR2 [**41**]. Multiple light-responsive elements have also been integrated together in a single strain. A dual-sensing optogenetic module was installed into *Pseudomonas aeruginosa* to sense both NIR and blue light, regulate intracellular levels of c-di-GMP and pattern biofilm formation based on exposure to each

light type [**42**]. The expression of the chromophore phycocyanobilin (PCB) and PCB-enabled red/green light photoswitchable two-component system allowed for multimodal transcriptional regulation in a *B. subtilis* biofilm [**43**]. Expression of the *E. coli* matrix protein CsgA fused with various peptide tags were transcriptionally activated via multiple different wavelengths of visible light, allowing for tunable control over *E. coli* matrix production and composition [**44**].

Optogenetics has enabled precise spatiotemporal control over bacterial gene expression and biofilm formation, with a growing list of available wavelengths and responsive cellular machinery. Future development will need to address delivery of light to engineered biofilms in natural target locations as well as advancing switching and multiplexing kinetics of light-activated transcriptional regulation.

**1.1.1.3. Functionalization of biofilms into engineered living materials.** During biofilm formation, individual motile bacteria adhere to a surface and begin to secrete exopolysaccharides, DNA, and proteins to form an extracellular matrix (ECM) that serves as a biofilm scaffold [**3, 45, 46**]. In particular, matrix proteins exist play a critical role, providing both macroscopic structure and distinct material properties that dictate cellular organization. Recent efforts are leveraging these proteins to transform biofilms into engineered living materials that can self-organize, regenerate, and interface with inorganic materials.

Biofilm matrix proteins secreted by the cell can self-assemble into long structures that form the basis for the biofilm ECM. These fibrils can be genetically modified to include different functional tags that imbue different material properties. The *E. coli* biofilm amyloid protein CsgA was genetically modified with various peptide domains to create

custom fusion proteins that could be produced by a host and self-assemble into ECM [**47**]. CsgA protein expression across multiple length scales has also been engineered to be driven by inducible gene circuits and quorum sensing, and later used to interface *E. coli* biofilms with inorganic materials such as quantum dots and gold nanoparticles [**48**]. Further tunable control over CsgA allowed for *E. coli* biofilms to serve as 3D pattered scaffolds for gold nanoparticles, creating resettable living pressure sensors [**49**]. The *B. subtilis* biofilm matrix amyloid protein TasA was functionalized with the adhesive mussel protein Mefp5 to transform *B. subtilis* biofilms into living and regenerating glues [**50**]. This strategy has been further expanded to genetically modify TasA with many different proteins and peptide domains, resulting in biofilms with tunable viscoelasticity and hydrogel properties that can be 3D printed into robust and self-healing materials [**51**].

Functionalization of biofilm matrix components has begun to transform biofilms into novel living materials with tunable physiochemical properties. Looking to the future, more work will be needed to fully characterize ECM properties over time in a natural target environment, as well as developing increased control over ECM monomer assembly.

### 1.1.2. Challenges for synthetic biology in biofilms

Compared to their domesticated laboratory counterparts, the genetic and biochemical profiles of cells in the biofilm state remain relatively uncharacterized, and often present conditions that are not amenable to current genetic circuit designs. Ongoing challenges

that must be considered for engineering biofilms include extracting microscopic and macroscopic measurements amongst millions of biofilm cells and contending with bacterial cell fate changes that occur during biofilm community development.

**1.1.2.1. Measurements of densely packed communities.** Biofilms are densely packed communities that contain millions of bacterial cells. The challenge remains to extract high-quality single cell measurements amidst the noise of heterogeneous biofilm cells. Special care must be taken in amplifying desired readouts and understanding the cellular dynamics and heterogeneity of the biofilm population. Recent methods have begun to address these challenges though use of microfluidics, microscopy, and high-throughput sequencing. Microfluidics have been used to overcome the noisiness arising from dense cellular through constricting biofilm growth to only a few cell layers thick. Using such devices, it has been observed that synthetic microbial consortia can coordinate across great length scales using quorum sensing genetic positive feedback loops [**52**]. Undomesticated *B. subtilis* biofilms were shown to spatiotemporally oscillate in growth and membrane potential in a microfluidic chamber [**5**]. Microfluidics have also enabled the study of diffusion-mediated interactions between spatially separate microbial communities [**53**]. To dissect biofilms with established 3D structure, light-sheet microscopy has been able to dissect *Vibrio cholerae* biofilms and track migration of individual cells within the developing community [**54**]. Finally, for determining bulk species composition in a community, high throughput sequencing has enabled quantification of relative abundance of microbiota in mucosal and luminal layers of the murine gut [**55**]. While these methods have provided critical biofilm-related measurements, live and *in situ* monitoring of biofilms in non-constrained natural conditions remains to be developed.

**1.1.2.2. Control over bacterial cell fate.** The majority of synthetic biology work is performed in bacterial cells during the exponential growth phase in order to take advantage of rapid cell replication and protein turnover. However, outside of the laboratory, most bacteria in nature do not appear to exist in this growth phase, instead transitioning to a variety of cell fates including stationary phase, cell death, and biofilm formation. These cellular fates and the cellular decisions that influence them are intertwined with metabolism and transcriptional networks, resulting in many genes being influenced by cell fate. When engineering biofilms, the cellular commitment to form a biofilm can be convoluted by other cell fate pathways, such as sporulation, dispersal, and localized cell death. This issue is further compounded by the lack of molecular and genetic tools that are designed to work in non-exponential growth phases. Even within biofilms, not all cells behave similarly in terms of matrix production and motility. In *Vibrio cholerae* biofilms, cells that grew at the biofilm front were transported from a founder population in a fountain-like pattern, whereas the remaining biofilm population near the substrate surface remained relatively immobile [**54**]. In *B. subtilis* biofilms, motile and sessile cells experience different transcriptional regulation of time spent in a lifestyle, suggesting that cells do not have to fully commit to biofilm formation [**56**]. Some species, including biofilm-forming *B. subtilis* also possess the propensity to form endospores in lieu of biofilms, resulting in a completely different transcriptomic profile [**57**]. Additionally, the current set of synthetic biology tools to engineer cells in stationary phase remain in their infancy. While some stationary phase promoters have been discovered and characterized, their numbers remain low and only have seen use in recombinant protein production where cells do not form biofilms [**58**]. Furthermore, the biological mechanisms occurring during stationary phase

are still being elucidated as non-growing bacteria have been shown to display a low but surprisingly constant protein production rate [**59**]. Cellular memory of stationary phase can also lead to a heterogeneous population, with the creation of persister cells [**60**].

### 1.1.3. Opportunities for engineered biofilms

Bacterial biofilms currently provide benefits for wastewater treatment and microbial fuel cells due to their ability to adhere, densely pack, and persistence in the environment [**61, 62**]. With improved understanding of biofilm biology and creation of new synthetic biology tools, biofilms are poised to advance synthetic biology efforts in medicine, manufacturing, and environmental remediation (Table 1).

**1.1.3.1. Cell-based medicine.** Within the gastrointestinal microbiota, probiotic and biofilm-forming species have been highlighted in recent studies as critical for healthy gut symbiosis. Engineering biofilms in this context could lead to the creation of new cell-based therapies where engineered bacteria could provide extended diagnostics and therapeutic delivery. Commensal *E. coli* Nissle (EcN) biofilms were engineered to outcompete pathogenic species, such as enterohemorrhagic *E. coli* , *Staphylococcus aureus*, and *Staphylococcus epidermis* through expression and secretion of the protease DegP [**63**]. Synthetic biosensing modules have created for EcN, allowing engineered strains to colonize the mouse gut, detect the inflammation marker tetrathionate, and genetically record inflammation exposure over months *in vivo* [**69**]. The EcN biofilm matrix itself has been employed as a modality to retain engineered cells in the mammalian gut. EcN curli fibrils were fused to the trefoil family of human cytokines and when delivered to a mouse gut, allowed for engineered EcN biofilms to entrain themselves in the mucosal later and influence

| Engineered biofilm applications | Description | Current Challenges | Enabling synthetic biology tools |
|---|---|---|---|
| Microbiome diagnostics | Biofilms as sentinel organisms in the mammalian gut to sense disease and pathogens | Quantifying readout from biofilm sensor, multispecies cooperation | Broad-spectrum species genetic transformation [**36, 37**], expansion of standardized genetic parts [**32, 33, 34**], biofilm ECM functionalization [**47, 48, 49, 50, 51**] |
| Microbiome therapeutics | Engineered biofilms regulate host microbiome through therapeutic production | Long term retention of engineered biofilm in gut, stationary phase gene circuit performance | Biofilm ECM functionalization [**47, 48, 49, 50, 51**], expansion of standardized genetic parts[**32, 33, 34**], engineered production of therapeutic and signaling biomolecules [**63, 64, 65**] |
| Biomanufacturing | Metabolic burden split across multiple cell populations within a biofilm for increased efficiency | Control over intraspecies cell fate, control over interspecies biofilm population distribution | Light-responsive optogenetic biofilm gene circuits [**39, 40, 41, 42, 43, 44**], broad-spectrum species genetic transformation [**36, 37**] |
| Novel biomaterials | Biofilm ECM with engineered biochemical properties to enable novel biomaterials | Stationary phase gene circuit performance, scale of material production | Light-responsive optogenetic biofilm gene circuits[**39, 40, 41, 42, 43, 44**], 3D bioprinting [**44, 49, 51**] |
| Environmental remediation | Removal of heavy metals and hazardous compounds, stored safely in the biofilm matrix | Biosensing of pollutants, long term control of engineered biofilm | Biofilm ECM functionalization [**47, 48, 49, 50, 51**], biofilm morphology control, novel biosensing gene circuits [**66, 67, 68**] |
| Biofouling prevention | Seeding surfaces with engineered biofilms to prevent attachment of microbial species | Long term control of engineered biofilm, multispecies cooperation | Light-responsive optogenetic biofilm gene circuits [**39, 40, 41, 42, 43, 44**], biofilm ECM functionalization [**47, 48, 49, 50, 51**] |

epithelial cell behavior [**64**]. Biofilm ECM was also used to coat probiotic *B. subtilis* cells, improving their gut mucoadhesion and bioavailability when delivered to both mouse and swine guts [**65**]. Other native biofilm-forming species could also serve as powerful tools, as many already interact and influence their host through secreted neuroactive molecules. *Providencia* bacteria living in the gut of *Caenorhabditis elegans* worms were found to modulate host sensory decision via tyramine production [**66**]. With special care taken to

understand and control immunogenicity and behavior, engineered biofilms could act as sentinel organisms in the mammalian gut and even deliver therapeutic payloads.

**1.1.3.2. Biomanufacturing.** Synthetic biology could enable the development of more efficient methods to synthesize biochemical compounds of interest. One common challenge with expressing multiple enzymes in a pathway is to minimize toxicity and metabolic burden on the host. Biofilms could potentially avoid this issue altogether through division of labor within its population. Such behavior occurs naturally during production of ECM components in *B. subtilis* biofilms, where cells cooperate to produce complementary products and contribute to the public goods pool of matrix [**23**]. Additionally, the biofilm ECM can be genetically modified to display specific affinities and crosslinking to transform the biofilm itself into a regenerating biomaterial with multimodal properties. Both *E. coli* and *B. subtilis* amyloid fibers where genetically modified to express proteins or peptide domains that allowed for the biofilm matrix to act as a renewable and robust biomaterial [**47, 50, 51**]. Additionally, these strategies can be combined in tandem with 3D printing to rapidly and precisely print biofilms into a desired shape. Utilizing division of labor in engineered biofilms will enable the next generation of biotechnologies for manufacturing sophisticated biochemical products and renewable biomaterials.

**1.1.3.3. Environmental remediation.** The ability to persist in natural environments makes biofilms an ideal platform for deploying engineered bacteria to directly mitigate and treat pollution. Bacterial biofilms already enjoy wide use in wastewater treatment where biofilms break down organic pollutants in controlled ponds. In more natural settings such as waterways and soil, synthetic biology could expand the role of biofilms as platforms for on-site remediation and upstream sequestration of pollutants. Indeed, recent studies have

established that biofilms are able to sequester pollutants from their environment. Rare earth elements can be captured by *E. coli* biofilms expressing genetically modified CgsA matrix protein [**67**]. Heavy metals such as mercury can also be sequestered by biofilms, as *E. coli* biofilms have been engineered to produce CsgA in the presence of mercury, which can immobilize mercury compounds in the fibrils [**68**]. Toxic halogenated compounds can also be degraded by biofilms, as *Pseudomonas putida* biofilms were engineered to express haloalkane dehalogenases, and this catalytic activity was further enhanced with tunable control over biofilm formation [**70**]. Biofouling on osmotic membranes have also been mitigated with use of programmable biofilms, as quorum-quenching E. coli biofilms were seeded into membrane materials and optogenetically controlled to prevent formation of biofilms from other species [**71**].

### 1.1.4. Future perspectives for synthetic biology in biofilms

Developing biofilms as next generation synthetic biology chasses holds great promise, yet important challenges remain to realize this vision. Current tools have only begun to address non-model biofilm-forming bacterial species and their complex social behaviors. Spatial heterogeneity and temporal dynamics associated with cell state and species composition in biofilms remain poorly understood. Furthermore, the environmental persistence of biofilms raises some concern about biocontainment, as biofilms have been associated with chronic infections and biofouling. Despite these challenges, the opportunity remains to co-opt the complex social behaviors of biofilms (e.g. cell-to-cell signaling, division of labor, and matrix production) for medicine, biomanufacturing, and environmental remediation. Additionally, basic scientific study of these processes could provide inspiration for

more sophisticated synthetic gene circuits beyond the biofilm context. In addition to intercellular coordination, the physical robustness and environmental persistence of biofilms could enable new living materials and robust deployment of engineered bacteria into target environments. These advances may also prove valuable beyond synthetic biology, impacting fields spanning materials science, ecology, and medicine. Overall, engineering individual bacteria has been instrumental to the advancement of synthetic biology thus far and the field is now poised to leverage bacterial biofilms for next generation synthetic biology applications

CHAPTER 2

# *In situ* measurement of biofilm energy metabolism

## 2.1. Background

While bacteria are single-celled organisms, they predominantly exist in nature within multicellular biofilm communities that exhibit complex emergent behaviors [**72, 73, 74, 75, 15, 76, 77, 78**]. This stands in contrast to free-swimming (planktonic) bacteria grown in rich laboratory conditions that most common microbiology assays utilize [**17, 18, 79**]. These methods of studying microorganisms have been practiced for decades and have been instrumental to fundamental discoveries in pathogenesis and microbial physiology. However, these microbiology techniques are often not readily applied to biofilms due to their architectural and compositional complexity [**15, 16**]. Biofilms are physiologically distinct from their planktonic counterparts and therefore require new methods to decipher their unique physiology. By developing tools to expand the field of microbiology towards the natural biofilm context, we will increase our understanding of the biology behind infection, ecological processes, bioreactor design, and other processes mediated by microorganisms [**17, 1, 18, 19**]. Furthermore, by gaining such insights into biofilm physiology, we will reveal new strategies for more effective antibiotic treatment in the context of disease. In particular, it has been recently proposed that multiple classes of bactericidal antibiotics produce harmful reactive oxygen species (ROS) that contribute to

their lethal effects [**80, 81**]. This surprising finding has now been found to apply to numerous planktonic bacterial species and multiple drug classes (especially aminoglycosides and $\beta$-lactams) [**82, 83, 84**].

These effects are thought to derive from multiple alterations to cellular respiration, central metabolism, and iron metabolism. Support for this hypothesis includes antibiotic tolerant clinical samples of pathogenic bacterial species which contain mutations in oxidative stress response and defense genes [**85, 86**]. However, this idea remains controversial and data has also been generated which limits the scope of this hypothesis. Specifically, recent investigations have found that antibiotics remain effective even in anaerobic conditions where ROS production is expected to be dramatically reduced [**87, 88**]. Thus, it is clear that the effects of antibiotics on the cell can include altered energy metabolism, but also that this relationship is more complex than originally thought.

In this context, one form of emergent behavior exhibited by biofilms is increased robustness in response to antibiotic treatment [**72, 15, 76, 79, 89, 90, 91, 92**]. Biofilms are thought to modulate aerobic energy metabolism and respiration during their development to cope with oxygen limitation caused by their dense growth. As such, one mechanism of their antibiotic resistance may involve the differentiation of the biofilm into distinct metabolic states. This might allow some members of the biofilm to survive metabolically-directed attacks where respiration is expected to play a role. Specifically, bacteria with reduced or altered energy metabolism-often termed persisters-are known to be more tolerant to antibiotic exposure [**72, 73, 93, 94, 95, 96, 97**]. Energy metabolism refers to the process of generating adenosine triphosphate (ATP) through glycolysis and aerobic respiration (Figure 2.1a). While the basic biochemical processes of energy metabolism

are well understood in planktonic bacteria, it remains unclear how bacteria alter their energy metabolism in biofilms. Understanding these biofilm-specific shifts in energy metabolism will be crucial to understanding how biofilms respond antibiotics which elicit ROS production as part of their lethality. Addressing this question requires quantitative measurements of biofilm energy metabolic responses during external perturbations, such as antibiotic treatment.

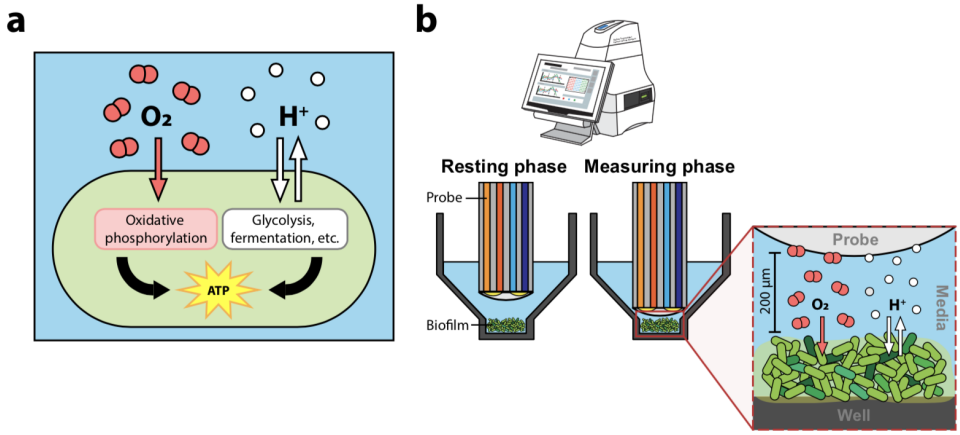


**Figure 2.1.** Overview of Seahorse XFe96 instrument setup for measuring biofilm energy metabolism. (a) Metabolic demands of the cell are met through oxidative phosphorylation and glycolysis to generate ATP through energy metabolism. Oxidative phosphorylation and acidification processes associated with glycolysis and fermentation can be quantified by measuring oxygen consumption and proton excretion rate, respectively. (b) Seahorse XFe96 alternates between a resting phase and a measuring phase. During the measuring phase, the probe lowers to create a transient micro-chamber of approximately 200 $\mu$m in height. The polymer-embedded fluorophores within the probe measure the oxygen and proton concentration as they are modified by the cells trapped within the microchamber. These oxygen and proton measurements are converted to oxygen consumption rate (OCR) and extracellular acidification rate (ECAR), respectively, by determining the rate of change of the fluorescent signal during the measurement phase (Figure 2.2).

The traditional methodology for measuring bacterial respiration is the Clark electrode, which is capable of reporting ambient oxygen concentration in a liquid using a

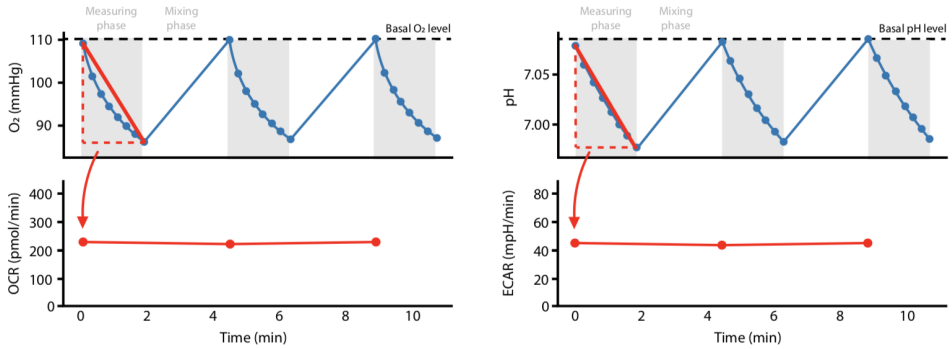


**Figure 2.2.** Calculation of OCR and ECAR from raw $O_2$ and pH measurements.Both oxygen consumption rates (OCR) and extracellular acidification rates (ECAR) are calculated based on the slope of the raw $O_2$ and pH values as they decrease over the measuring phase, during which the probe lowers to create a transient microchamber. This is followed by a mixing phase where the probe returns to its original position and gently introduces new media to the cells to bring $O_2$ and pH levels back to their baseline.

catalytic platinum surface. While Clark electrodes are able to effectively measure local oxygen levels, they are slow, low-throughput, and unable to record time-resolved measurements [**98, 99**]. More importantly, Clark electrodes do not measure extracellular acidification, an important measure of anaerobic processes such as fermentation, and thus exclude these critical aspects of metabolism. Furthermore, because measurements are not time-resolved, Clark electrodes cannot be used to measure in situ metabolic changes in response to perturbations such as antibiotics. Thus, a new method is needed for biofilm-specific measurements of energy metabolism during antibiotic perturbations. The Agilent Seahorse XFe96 is a high-throughput instrument that provides insight into cellular metabolism by simultaneously measuring oxygen consumption rate (OCR) and extracellular acidification rate (ECAR). OCR acts as a proxy for cellular respiration whereas ECAR reflects proton efflux through acidification processes such as glycolysis and lactate production [**91**]. While Seahorse experiments are traditionally performed on mammalian cells

[**98, 99**], we reasoned that we could also capture metabolic changes in biofilms as aerobic respiration and glycolysis are biochemically conserved.

As a proof-of-concept, we applied our method to biofilms of undomesticated *Bacillus subtilis*. We show our method can reliably and reproducibly track energy metabolic dynamics over time. In particular, we observe that biofilms generate higher levels of acidification compared to planktonic cells, suggesting a biofilm-specific increase in acidifying metabolic processes such as glycolysis and fermentation, despite comparable levels of respiration. Additionally, our data points to co-regulation between oxygen consumption and acidification in biofilms during antibiotic perturbations, which may contribute to community antibiotic resistance. Our approach will enable better understanding of metabolic dynamics in biofilms, advancing research in both basic microbiology and biomedical approaches to overcome emergent antibiotic resistance.

## 2.2. Results

### 2.2.1. High-throughput method for tracking biofilm metabolic dynamics

We developed a high-throughput method using the Agilent Seahorse XFe96 metabolic analyzer to measure energy metabolism during biofilm development (Figure 2.1b). The device alternates between resting and measuring phases based on a user-defined protocol. During the resting phase, the probe introduces oxygen into the well through gentle mixing. During the measuring phase, the probe lowers to confine the biofilm to a microchamber where oxygen and pH are measured by embedded fluorophores (Figure 2.1b). After the measuring phase, the probe returns to its starting position, allowing oxygen

and pH to return to their baseline levels. The linear slope of the oxygen and pH measurements are used to calculate OCR and ECAR (Figure 2.2). Since the device creates a transient microenvironment close to the surface where the biofilm is adhered, OCR and ECAR measurements can accurately monitor biofilm energy metabolism. Our method thus provides insight into energy metabolism during biofilm development by quantifying levels of oxidative phosphorylation and acidification over time.

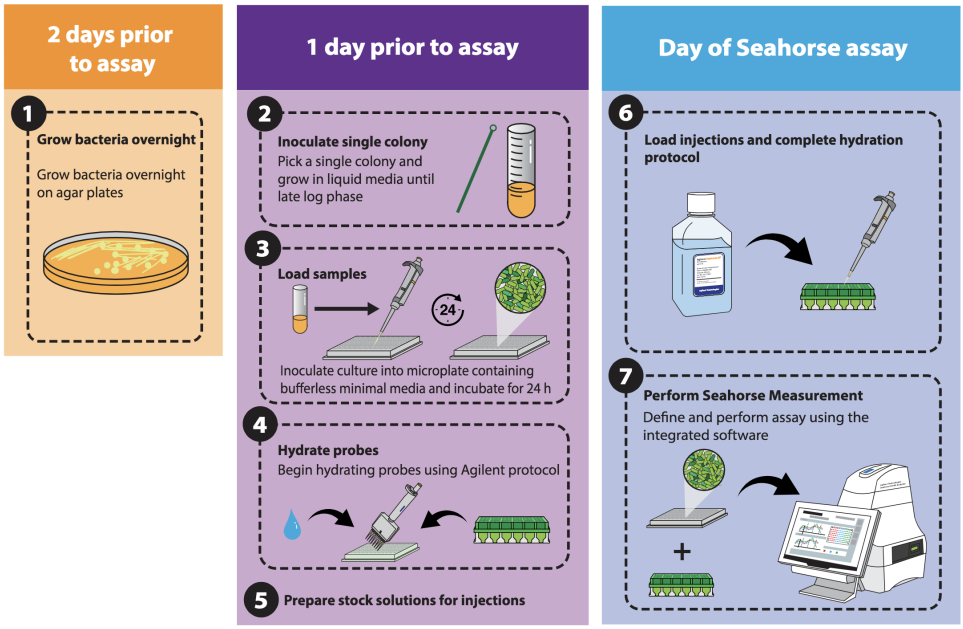


**Figure 2.3.** Schematic of assay protocol for measuring biofilm energy metabolism. Beginning two days prior to assay: (1) culture bacteria overnight on LB agar plates; (2) inoculate a single colony for growth in LB broth until late log phase one day prior to assay; (3) load samples in the microplate and incubate for 24 hours to allow biofilm formation; (4) begin hydrating probes using the Agilent-specified protocol; (5) prepare stock solutions, such as antibiotics, for chemical injections; (6) finish hydrating probes and loading injections; and finally (7) perform Seahorse measurement and data analysis.

Seahorse is typically viewed as a mammalian metabolic analysis tool and it has never been utilized to study bacterial biofilms. We were inspired by recent studies that adapted

the assay to measure respiration in planktonic bacteria [**84**]. These studies showed that aminoglycosides are capable of producing transient increases in OCR over several hours. However, these studies were performed on planktonic bacteria that lack the potential for emergent control of metabolism during biofilm development. We therefore established a protocol for measuring in situ energy metabolism over long-term development in the natural biofilm context (Figure 2.3). The method can accommodate up to 20 distinct mutant strains grown in triplicate within the interior of the 96-well microplate over the course of 12 hours. In addition, each well contains an integrated injection system capable of delivering up to 4 different drug or nutrient perturbations during the experiment. Our protocol provides a simple and flexible method for quantifying energy metabolic changes in biofilms over time during antibiotic treatment.

### 2.2.2. Reproducible, time-resolved measurements of biofilm energy metabolism

We sought to validate biofilm formation within the microplate by comparing an undomesticated *B. subtilis* wild type strain (3610) to a non-biofilm forming mutant (3610 ΔsinI). Since SinI modulates the activity of SinR, a transcriptional regulator of genes essential for biofilm formation, the 3610 ΔsinI mutant cannot form biofilms and is constitutively planktonic35. Biofilm formation begins when planktonic bacteria adhere to a surface and proliferate, eventually producing an extracellular matrix that encapsulates the biofilm (Figure 2.4a). We confirmed that 3610 is capable of forming biofilms in the microplate within the experimental timeframe using a crystal violet stain to report extracellular matrix content. When we compared 3610 and 3610 ΔsinI, we found that 3610 displayed

significantly higher (n = 3, Mann-Whitney U-test, $p < 0.05$) crystal violet absorbance compared to the non-biofilm forming mutant, confirming biofilm formation in the microplate (Figure 2.4b). After validating formation during the experimental time-frame, we could then move toward analyzing biofilm energy metabolic changes over time.

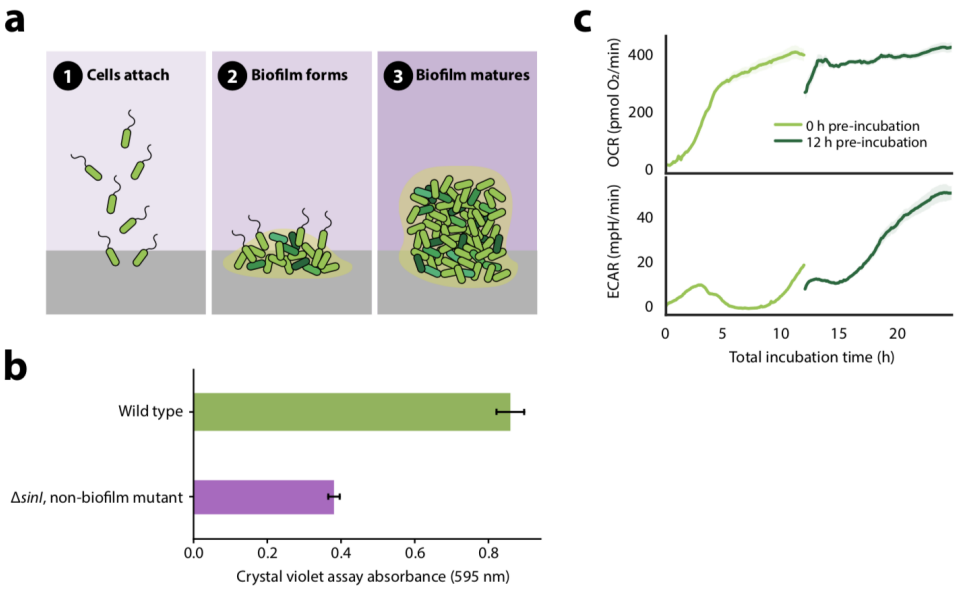


**Figure 2.4.** Biofilm formation and development in the microplate. (a) Following inoculation, planktonic bacteria adhere to microplate surface and begin initial attachment. After attachment, biofilm cells proliferate and produce a dense extracellular matrix (yellow). Finally, after 12-24 hours, a mature biofilm is produced. (b) Biofilm formation assay with crystal violet staining using undomesticated B. subtilis wild type (3610) and a non-biofilm forming mutant (3610 ΔsinI) shows higher absorbance for 3610 (error bars ±SE, n = 3, Mann-Whitney U-test, $p < 0.05$). (c) Time-resolved measurements of OCR (pmol/min) and ECAR (mpH/min) during biofilm formation. The 24-hour time course was assembled using parallel experiments where pre-incubation time was reduced to 12 hours (dark green) or 0 hours (light green). Bolded mean is shown with standard error (n = 6).

In order to determine how altered metabolic state affects antibiotic response, we first tracked energy metabolism during biofilm formation to determine the relevant changes that occur. We gathered time-resolved measurements of OCR and ECAR during the

24-hour process of biofilm formation beginning from inoculation (Figure 2.4c). Since measurement times are limited to 12 hours, we combined two parallel experiments where pre-incubation time was reduced to 12 hours (dark green) or 0 hours (light green) to form a continuous, 24-hour trace. The observation that multiple parallel runs can be stitched together to form a continuous trace indicates that growth conditions within the Seahorse instrument are qualitatively similar to that of the incubator, and assay measurements are therefore likely to be physiological. These long-term development traces show a reproducible increase in ECAR during the later stages of biofilm formation (Figure 2.4c). The increase in ECAR late in biofilm maturation suggests acidification increases as a result of biofilm formation, perhaps due to an increase in anaerobic metabolic processes such as glycolysis and fermentation as oxygen becomes limiting within the interior of the biofilm.

### 2.2.3. Biofilm-specific differences in energy metabolism compared to the planktonic context

To confirm that the late-onset increase in ECAR is a biofilm-specific change, we next examined differences in energy metabolism between 3610 and 3610 ΔsinI. Following a standard 24-hour pre-incubation to establish the biofilm, measurements of OCR and ECAR were taken for planktonic and biofilm strains over a period of four hours (Figure 2.5a). As expected, we found that biofilms showed reproducibly higher ECAR while displaying comparable levels of OCR relative to planktonic strains (Figure 2.5a). Furthermore, quantification of this data at the 4-hour time-point revealed that the ratio of OCR and ECAR are shifted toward acidification in biofilm communities (Figure 2.5b,c). Interestingly, despite higher rates of acidification in biofilms, the pH of biofilm wells remained

slightly higher than non-biofilm wells (Figure 2.6). The presence of both high acidification rates and a more alkaline pH suggests the existence of a compensatory process in the biofilm that is absent in the planktonic context. To further confirm these findings, we repeated these experiments in a laboratory-adapted strain of B. subtilis (168) and again observed reduced acidification in the laboratory-adapted strain (Figure 2.7). Thus, these data confirm that the late-onset increase in ECAR is a biofilm-specific change in energy metabolism.

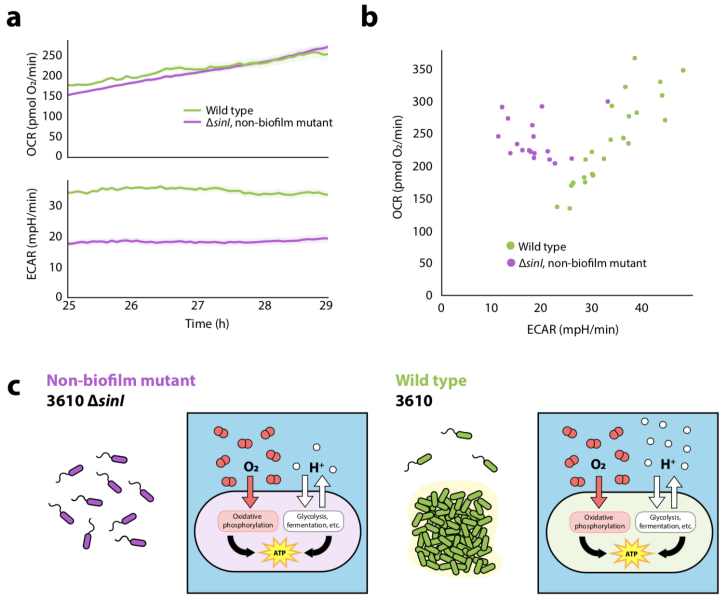


**Figure 2.5.** Differences in energy metabolism between biofilm and planktonic *B. subtilis*. (a) Measurements of OCR and ECAR in biofilm wild type (3610, green, n = 23) and non-biofilm mutant (3610 ΔsinI, purple, n = 18) strains of B. subtilis. Mean is shown with standard error. (b) Scatterplot of OCR and ECAR at the 4-hour time point for biofilm wild type (3610, green, n = 23) and non-biofilm mutant (3610 ΔsinI, purple, n = 18) strains of B. subtilis. ECAR is significantly lower in the non-biofilm mutant (Mann-Whitney U-test, p < 1E-6), while OCR is not (Mann-Whitney U-test, p = 0.36). (c) Overall level of ECAR is lower in the non-biofilm mutant (3610 ΔsinI, shown in purple) compared to the wild type biofilm strain (3610, shown in green) of B. subtilis reflecting higher levels of respiration and acidification in biofilms.

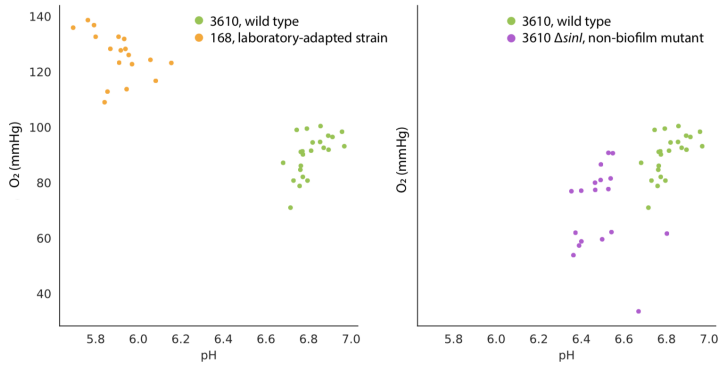


**Figure 2.6.** Biofilms have a more alkaline pH than planktonic cells despite higher measured rates of acidification. (a) Scatterplot of pH and O2 (mmHg) at the 4-hour time point in biofilm wild type (3610, green, n = 23) and non-biofilm mutant (3610 ΔsinI, purple, n = 18) strains of B. subtilis. (b) Scatterplot of pH and $O_2$ (mmHg) at the 4-hour time point for undomesticated, biofilm-forming strain (3610, green, n = 23) and domesticated, non-biofilm laboratory strains (168, orange, n = 18) of *B. subtilis*.

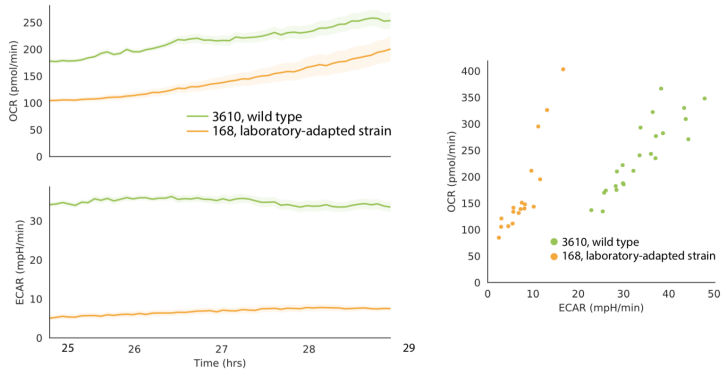


**Figure 2.7.** The reduction in acidification for planktonic cells compared to biofilms is also observed using a laboratory-adapted strain (168). (a) Measurements of OCR and ECAR in the undomesticated, biofilm-forming strain (3610, green, n = 23) and domesticated, non-biofilm laboratory strains (168, orange, n = 18) of B. subtilis. Mean is shown with standard error. (b) Scatterplot of OCR and ECAR at the 4-hour time point for undomesticated, biofilm-forming strain (3610, green, n = 23) and domesticated, non-biofilm laboratory strains (168, orange, n = 18) of *B. subtilis*.

**2.2.3.1. pH differences between the biofilm and planktonic context.** We also investigated how biofilm and planktonic energy metabolism was effected by extracellular

pH. Previous studies have found that pH conditions outside of a cell's preferred pH range (e.g. pH 6.5 to 7.5 for neutrophiles) can disrupt ability to maintain functional proton motive force (PMF) and thus respiration [**100, 101, 102**]. Using unbuffered MSgg, we created several pH conditions (pH 3.0, 4.1, 4.6, 5.1, 5.6, 6.1, 6.6, 7.1, 7.6, 8.1, and 8.6) and inoculated either WT or ΔsinI in the Seahorse microplate. We then compared the average OCR and ECAR rates of both strains across pH conditions to determine how the bacterial lifestyles adapted their energy metabolism to different pH conditions (Figure 2.8).

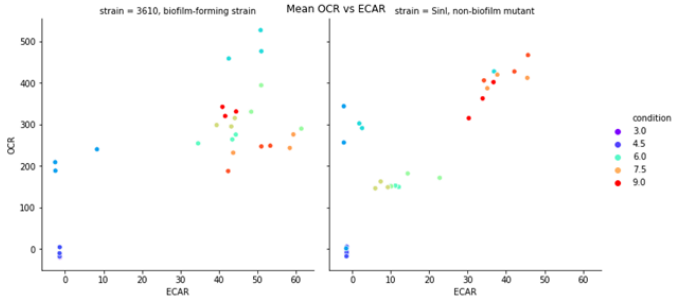


**Figure 2.8.** OCR vs. ECAR for WT and ΔsinI across various pH conditions. Left, Measurements of average OCR vs. ECAR in the undomesticated, biofilm-forming strain (3610, n = 3). Right, Measurements of average OCR vs. ECAR in the planktonic strain (ΔsinI, n = 3) of B. subtilis.

Interestingly, we observed that the biofilm-forming 3610 had higher average OCR and ECAR overall across pH conditions compared to planktonic ΔsinI, suggesting perhaps that biofilm formation helped enable energy metabolism even in non-ideal pH conditions. To directly probe this, we utilized a feature of the Seahorse platform and ECAR calculation where the instrument directly measures extracellular pH. We then compared the initial starting pH (where each strain was inoculated into) and the end pH (to determine the effects of growth and metabolic activity). Surprisingly, we found that when starting at pH

5.6 to 8.1, WT biofilms ended at an extracellular pH of approximately 7 whereas ΔsinI culture end pH mainly tracked with initial pH (Figure 2.9).

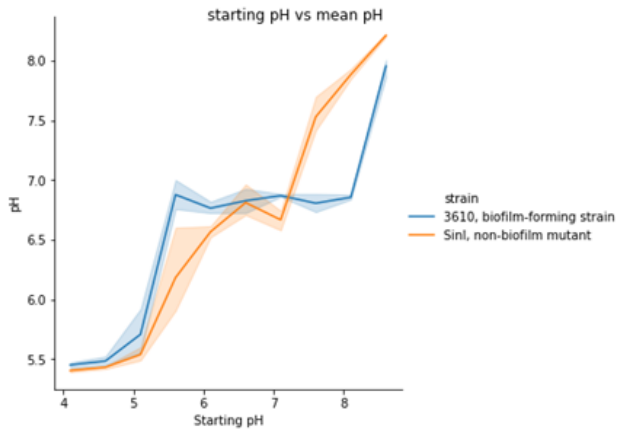


**Figure 2.9.** End vs. starting pH for WT and ΔsinI across various pH conditions. Strains were grown in the Seahorse Xe96 at pH 3.0, 4.1, 4.6, 5.1, 5.6, 6.1, 6.6, 7.1, 7.6, 8.1, and 8.6 in bufferless MSgg. Extracellular pH values were obtained from the raw ECAR Seahorse data. Strains: NCIB 3610 WT and ΔsinI, n=3 each.

This results suggested that biofilm development allowed for some kind of pH regulation over the biofilm extracellular space, and would serve as inspiration for future studies in Chapter 3.

### 2.2.4. Metabolic responses to antibiotic treatment are coordinated in biofilms

Motivated by the difference in ECAR, we next wanted to determine whether biofilms differentially respond metabolically to antibiotic perturbations. In our assay, we administered a variety of antibiotic types at an equivalent inhibitory dose to resolve differences in metabolic response independent of lethality. After four hours of baseline measurement, we used the integrated injection ports to administer antibiotics and assayed metabolic response by capturing the resulting dynamics of ECAR and OCR (Figure 2.10a). We

quantified metabolic responses by using the mean of a one-hour window from the baseline measurement before antibiotic injection (initial value) and the mean of a one-hour window nine hours after antibiotic injection (final value) to calculate percent change (Figure 2.10b). We assembled a broad panel of antibiotics targeting cell wall synthesis, nucleic acid synthesis, and protein synthesis (Figure 2.10c). In particular, we included several aminoglycosides (kanamycin, neomycin, and spectinomycin) which have been reported to produce energy metabolic changes as part of their lethality [**103**]. Thus, these experiments would allow us to not only demonstrate the reliability of our method, but also to determine whether the reported metabolic response to antibiotics is preserved in the natural biofilm context.

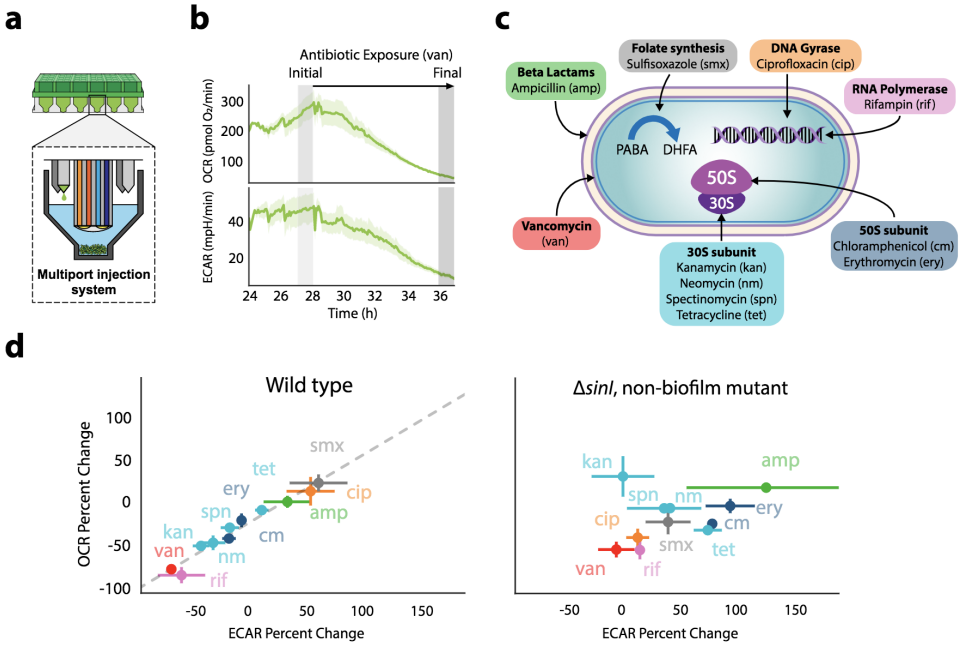


**Figure 2.10.** Planktonic and biofilm cells have different metabolic responses to antibiotic perturbations. (a) Sensor cartridges contain four integrated injection ports per well. (b) We injected each antibiotic at the 4-hour time point of a 12-hour experiment. To quantify metabolic response, we took the means of the one-hour window before antibiotic injection (initial value) and nine hours after antibiotic injection (final value) to calculate the percent change. (c) Panel of antibiotics used in this study organized by mode of action. (d) Scatterplot of mean ΔOCR (%) versus mean ΔECAR (%) to visualize metabolic response for biofilm (3610, n = 6 for all except ery, n = 9 and nm, n = 3) and non-biofilm mutant (3610 ΔsinI, n = 3) strains of B. subtilis (error bars ±SE). Gray line for wild type indicates linear fit to experimental data ($R^2 = 0.98$) which is not observed in the ΔsinI non-biofilm mutant ($R^2 = 0.37$).

We administered the panel of antibiotics and measured the metabolic response (OCR and ECAR) in each case. For each antibiotic perturbation, we calculated the percent changes for OCR and ECAR, ΔOCR and ΔECAR respectively, for 3610 and 3610 ΔsinI (Figure 2.10d). We observed that the biofilm antibiotic responses followed a linear relationship ($R^2 = 0.98$) between mean ΔOCR and mean ΔECAR, suggesting that these energy metabolic responses to antibiotics are co-regulated in biofilms. In contrast, the

planktonic OCR and ECAR responses were much less linear ($R^2 = 0.37$). In particular, by quantifying the residuals for each antibiotic, we found that the strongest outliers from the expected linear relationship were aminoglycosides with increased ΔOCR compared to the biofilm context (Figure 2.11). This finding is consistent with previous studies which reported that aminoglycosides increase aerobic respiration as part of their lethality [**103**]. These data imply that biofilms co-regulate oxidative and acidification processes during antibiotic treatment which may contribute to their antibiotic resistance, especially in the case of aminoglycosides. Important future work will involve unraveling the mechanisms by which biofilms are capable of regulating their energy metabolism to resist these metabolically-directed attacks.

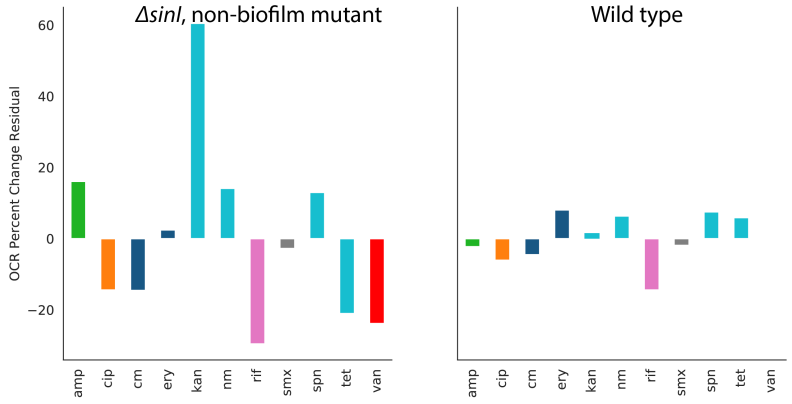


**Figure 2.11.** Comparison of residuals from a linear regression between mean ΔOCR and mean ΔECAR. The wild type 3610 strain has a better overall fit ($R^2 = 0.98$) than the non-biofilm mutant ($R^2 = 0.37$).

## 2.3. Discussion

Biofilm formation and energy metabolism have been linked in multiple model systems [**104, 105, 106, 107**]. In particular, it is known in the opportunistic pathogen *Pseudomonas aeruginosa* that bacterial community structure is linked to respiration and electron acceptor availability [**107**]. In the case of *Bacillus subtilis*, it has been similarly suggested that aerobic respiration limitation is associated with the transition to multicellularity in biofilm communities [**106**]. Our results suggest respiration levels are comparable in biofilms and planktonic cells, while extracellular acidification associated with glycolysis and fermentation is higher in biofilms. These findings reflect increased heterogeneity of metabolic states in biofilm communities. Based on the literature, we hypothesize that the non-growing interior regions of the biofilm (which lack access to oxygen) perform acidifying fermentation while the actively growing peripheral regions perform oxidative phosphorylation [**16**]. By generating heterogeneity of metabolic states within the community, biofilms are thus capable of maintaining high rates of respiration while also performing alternative energy metabolism, such as fermentation. As a result, biofilms may have mechanisms to coordinate changes in oxygen consumption and extracellular acidification that could be utilized during antibiotic exposure. Such co-regulation of aerobic respiration and glycolytic activities in biofilms may play a role in antibiotic resistance, especially in the case of aminoglycosides which have been reported to modulate respiration as part of their lethality. In agreement with this, aminoglycosides elicited an increase in respiration when comparing against the biofilm antibiotic response. We observed the reported respiration effects of antibiotics for planktonic bacteria but not in the natural biofilm context, and it therefore appears that biofilms exhibit an altered

energy metabolic response to antibiotics. These findings may serve to explain why there have been differing descriptions of the role of aerobic respiration in antibiotic resistance thus far. Future work will involve determining the mechanisms by which bacterial biofilm communities co-regulate their energy metabolic processes to evade these effects of antibiotics. For example, it is possible that disrupting biofilm-specific acidification may provide a means to render biofilms more susceptible to antibiotics. In this context, the high-throughput nature of our method is compatible both with genetic studies using deletion libraries as well as chemical small molecule screens. Our method will enhance basic microbiology studies toward understanding the emergent metabolic behaviors of the most pervasive bacterial lifestyle, while also accelerating biomedical research to combat antibiotic resistant biofilm-mediated infections.

## 2.4. Methods

### 2.4.1. Strains

| Strain | Organism | Genotype |
|---|---|---|
| Wild type | *B. subtilis* NCIB 3610 | |
| Δ*sinI* | *B. subtilis* NCIB 3610 | *sinI*::neo |

### 2.4.2. Growth conditions

Bacteria were grown in Luria-Bertani (LB) rich media overnight and or grown day-of experiment and seeded into MSgg media. Biofilms in fully buffered conditions were grown in standard MSgg, which contains 100 mM MOPS, 5 mM potassium-phosphate buffer (pH 7), 2 mM MgCl2, 700 $\mu$M CaCl2, 50 $\mu$M MnCl2, 100 $\mu$M FeCl3, 1 $\mu$M ZnCl2, 2 $\mu$M

thiamine HCl, 0.5% (v/v) glycerol, and 0.5% (w/v) monosodium glutamate. Biofilms in minimally buffered conditions were grown in modified MSgg, which contains 1 mM MOPS, 5 mM potassium-phosphate buffer (pH 7), 2 mM MgCl2, 700 $\mu$M CaCl2, 50 $\mu$M MnCl2, 100 $\mu$M FeCl3, 1 $\mu$M ZnCl2, 2 $\mu$M thiamine HCl, 0.5% (v/v) glycerol, and 0.5% (w/v) monosodium glutamate. The glutamate stock which was made fresh day of experiment.

### 2.4.3. Seahorse assay protocol

Two days prior to the assay, we grew Bacillus subtilis strains overnight on LB agar at 37°C. One day prior to assay, we inoculated a single colony into LB broth and grew until the culture reached late log-phase growth (approximately OD600 nm 0.8 in the case of Bacillus subtilis). Next, we loaded samples by inoculating 1 $\mu$L culture into 149 $\mu$L bufferless Msgg (minimal media excluding buffers) into the microplate (Agilent) and kept in a static incubator for 24 hours at 30°C to allow biofilm formation. After loading samples, probes were hydrated according to the Agilent-specified protocol and stock solutions were prepared for injection, if required. On the day of the assay, we hydrated probes to completion and loaded injections according to the Agilent-specified protocol. Finally, the Seahorse measurement was defined and performed using the integrated software.

### 2.4.4. Biofilm formation assay

Biofilm formation assays were conducted following the completion of the Seahorse assay. The wells were rinsed twice with distilled water to remove non-adherent planktonic bacteria. Cells were fixed using 0.1% (w/v) crystal violet stain for 15 minutes. Stain was removed and wells were washed with distilled water twice. Crystal violet solution was

resuspended in ethanol and optical density was measured at 595 nm using a microplate reader (TECAN). To correct the background staining of crystal violet, the mean optical density at 595 nm of the negative control was subtracted from the mean optical density at 595 nm of biofilm formation by Bacillus subtilis.

### 2.4.5. Statistical calculations

Statistics were calculated using Scipy 1.1.0 in Python 3.6. To determine significance a non-parametric Mann-Whitney U-test was used, as a Shapiro-Wilk test indicated that the assumption of normality could not be made. Linear regression was performed using a linear least-squares regression. Plots were made using Matplotlib 3.0.0, and Pandas 0.23.4. For each replicate percent change was calculated from the mean of a one-hour window (initial value) and the mean of a one-hour window nine hours later (final value). After calculation of percent change the mean and standard error of the replicates was determined.

CHAPTER 3

# Active pH control in biofilms

## 3.1. Background

Bacteria inhabit a diverse range of environmental niches and engage in specific lifestyles to thrive within their local environment. In controlled laboratory conditions, bacteria primarily exist as planktonic (free-swimming) individuals whereas in natural environments bacteria often form sessile, multicellular communities known as biofilms [**1, 2**]. Biofilms create a densely packed local environment with extracellular matrix (ECM) [**3, 4**] that can give rise to complex emergent behaviors such as cell-to-cell signaling [**5, 6**], macroscopic spatiotemporal organization [**7, 8, 9**], and metabolic remodeling [**10, 11**]. Furthermore, the biofilm structure creates a diffusion barrier and resulting local concentration gradients, producing habitat diversity and increased resilience against antibiotics [**12, 13, 14**]. Thus, the biofilm state confers advantages to individual bacteria for persisting in their local environment that are unavailable to planktonic cells.

However, this dense cellular proliferation can also create unique metabolic challenges. In particular, rapidly growing biofilm bacteria engage in overflow metabolism where carbon is not completely oxidized via respiration and instead only partially oxidized via fermentation [**108, 109**]. This counter-intuitive strategy enables rapid growth by circumventing production of energy-intensive respiratory enzymes while using increased metabolic flux into fermentation pathways that produce excretable byproducts such as lactate

and acetate [**108, 110**]. In the densely packed and diffusion-limited biofilm environment, these acidic metabolites can accumulate and exacerbate metabolic stress on sessile biofilm cells [**111, 112**]. Importantly, excessively acidic conditions disrupt a cell's ability to maintain functional proton motive force (PMF), increase energy expenditure for maintaining intracellular pH homeostasis, and impede growth via degradation of enzymatic activity [**100, 101, 102**]. These effects may be particularly pronounced for Gram-positive bacteria that possess only a single cell membrane where the electron transport chain (ETC) is directly exposed to extracellular pH [**113**]. Consequently, biofilm cells must maintain pH homeostasis against increasingly acidic conditions that arise during biofilm development.

These acidification challenges are usually masked by buffered laboratory media employed to stabilize the pH environment for optimal bacterial growth [**114, 115**]. In contrast, bacteria in nature persist in settings that often lack robust buffering systems and face significant pH variation from environmental sources and heterogeneous mixing [**1, 2, 116**]. Indeed, natural environments such as the soil, ocean, and human gastrointestinal tract exhibit pH gradients that can influence microbial population composition and behaviors [**117, 118, 119, 120**]. It therefore remains unclear how biofilms maintain growth, PMF, and pH homeostasis against the acidification associated with biofilm growth in such minimally buffered environments. To approach this question, we established a biofilm model system with a minimally buffered media that preserves cellular growth while enabling measurement of the local pH. Our findings reveal that biofilms use an active pH regulation mechanism to facilitate biofilm development in minimally buffered conditions.

## 3.2. Results

### 3.2.1. Modulation of extracellular pH by *B. subtilis* biofilms in minimally buffered conditions

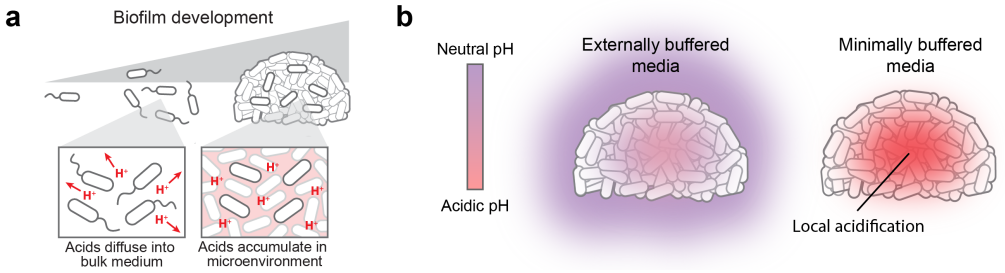


**Figure 3.1.** Emergence of extracellular acidification during biofilm development. a, Schematic showing biofilm development and acidification of the local environment. b, Schematic showing measurements of extracellular pH in biofilms across different buffered environments, using a cell-impermeable pH reporter, BCECF free acid.

In the planktonic lifestyle, acidic metabolic byproducts produced through via overflow metabolism can freely diffuse into the bulk medium, thereby minimizing local acidification (Figure 3.1a) [**121, 122**]. In contrast, in densely packed bacterial communities known as biofilms, acidic metabolic byproducts accumulate in the local environment due to limited diffusion (Fig. 1a) [**123, 124, 125**]. In buffered laboratory media, such excessive acidification is counteracted by an external chemical buffer such as MOPS (Figure 3.1b, left) [**114, 115**]. The external chemical buffer allows densely packed biofilms to continue proliferating despite the accumulation of acidic metabolic byproducts. While experimentally convenient, the common use of external chemical buffers in biofilm experiments provokes the question of how undomesticated biofilms in nature cope with largely minimally buffered conditions (Figure 3.1b, right). Accordingly, we wondered whether biofilms have active strategies for mitigating the accumulation of acidic metabolic byproducts.

To approach this question, we established a minimally buffered experimental system capable of tracking extracellular pH during biofilm development. Specifically, we modified the defined media MSgg, commonly used to grow Bacillus subtilis NCIB 3610 biofilms, by systematically varying each buffer component while monitoring growth and biofilm development. We found that reducing the MOPS buffer concentration from 100 mM to 1 mM while maintaining standard potassium-phosphate buffer levels permitted biofilm growth and development without measurable defect (Figure 3.2, 3.3).

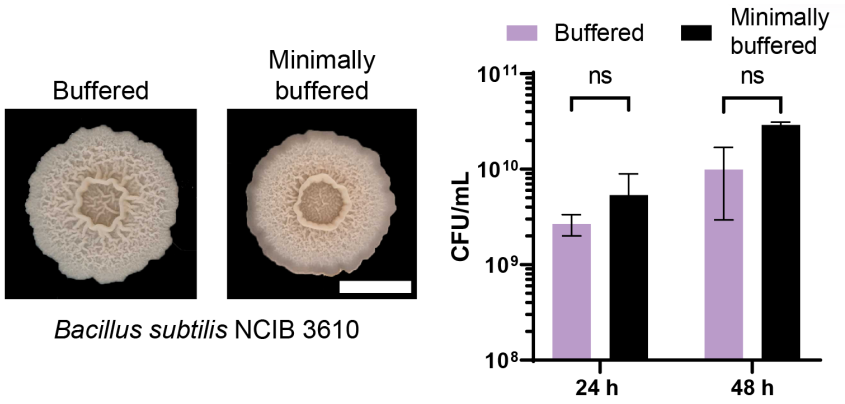


**Figure 3.2.** *B. subtilis* NCIB 3610 biofilms grown in fully and minimally buffered MSgg media. Left, images of Bacillus subtilis NCIB 3610 grown on fully buffered MSgg media containing 100 mM MOPS vs. minimally buffered. Images correspond to biofilms at 48h, scale bar represents 5 mm. Right, CFU measurements of 3610 biofilms grown on buffered and minimally buffered MSgg. Biofilms were harvested at 24 and 48 h. Images correspond to biofilms at 48h, scale bar represents 5 mm. Data: mean ± std, n=3 technical replicates. Strain: NCIB 3610.

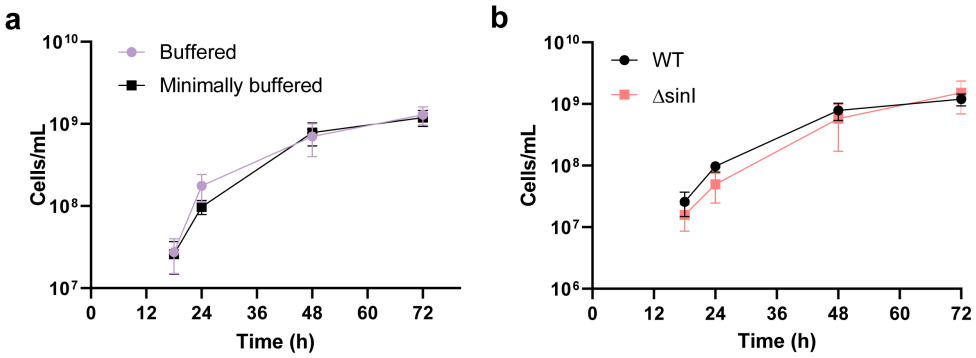


**Figure 3.3.** Biofilm growth measurements in buffered (100 mM MOPS) and minimally buffered (1 mM) MSgg media over time. a, Biofilm cell density measurements over time. Biofilms were harvested in protocol outlined in Methods section. Data: mean ± std, n=3 technical replicates. b, 3610 WT and ΔsinI cell density measurements in minimally buffered (1 mM MOPS) MSgg. Both strains were harvested in protocol outlined in Methods section. Data: mean ± std, n=3 technical replicates.

To track biofilm pH, we utilized 10 uM BCECF free acid, a cell-impermeable dye whose fluorescence linearly scales with the physiologically relevant pH range 5 to 9 (Figure 3.4). We could then grow 3610 WT biofilms in static liquid MSgg (minimally buffered vs. fully buffered) with 10 uM BCECF free acid at 30°C to form liquid-air pellicles and track BCECF fluorescence over 68 h. This experimental system permits the dynamic measurement of extracellular pH during biofilm development in a minimally buffered environment.

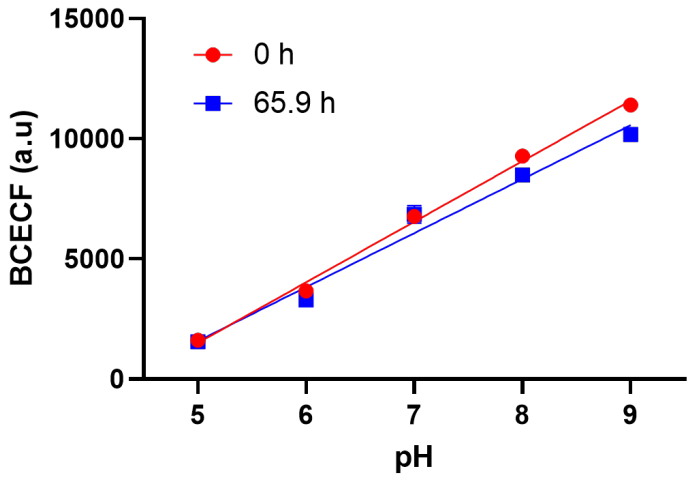


**Figure 3.4.** BCECF free acid fluorescence over extracellular pH. BCECF free acid was added into MSgg media at 10 uM concentration and measured at 490/535 nm Ex/Em, Red data points represent BCECF measurements taken at 0 h (directly after media preparation) and blue data points represent BCECF measurements taken after approximately 65.9 h in MSgg media incubated at 30°C. Both data sets were fitted with a simple linear regression with $R^2 = 0.94$ in both cases. For each experiment, a BCECF standard curve was used to internally calibrate BCECF signal to pH and subsequently convert measured BCECF fluorescence during biofilm growth to extracellular pH.

Using this experimental system, we found that *B. subtilis* displays a striking two-phase pH dynamic during biofilm development that is completely masked in standard MSgg media (Fig. 1d). Specifically, we observed an initial acidification phase (15.0 ± 0.3 h) followed by an extended alkalinization phase (31.2 ± 0.5 h) that ultimately returns the pH to the neutrophile range (Figure 3.6a). Biofilms acidify to approximately pH 5.5 at an average rate of 0.06 ± 0.0008 pH/h and alkalinize back to pH 6.9 at an average rate of 0.03 ± 0.0005 pH/h (n=42). We verified that this dynamic is not due to changes in growth rate (Figure 3.3a) and observed that the alkalinization phase occurred during latter biofilm development. Furthermore, we found that a planktonic mutant strain (3610 ΔsinI) was unable to return to neutral (one-sided t-test, n=42, $p<0.000001$) due to a complete lack of the alkalinization phase (Figures 3.6b, 3.7). As before, we verified that the absence of alkalinization was not due to differences in growth (Figure 3.3b). Thus, we concluded that the two-phase pH dynamic is specific to the biofilm lifestyle.

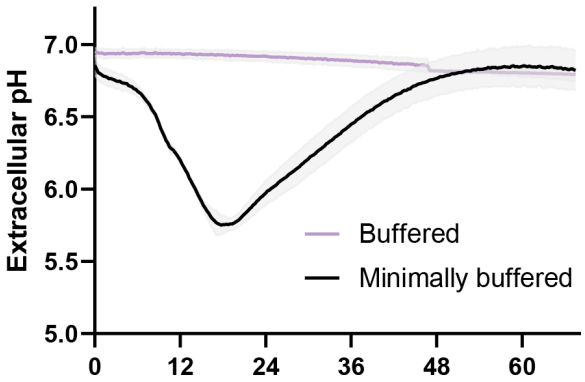


**Figure 3.5.** Extracellular pH tracked over time with NCIB 3610 biofilms in buffered (100 mM MOPS) and minimally buffered (1 mM MOPS) MSgg. Biofilms were grown statically at 30°C. Extracellular pH is calculated from the fluorescence intensity (535 nm) of a cell-impermeable pH reporter, BCECF free acid, over time. Data: mean ± std, n=4 technical replicates. Strain: NCIB 3610.

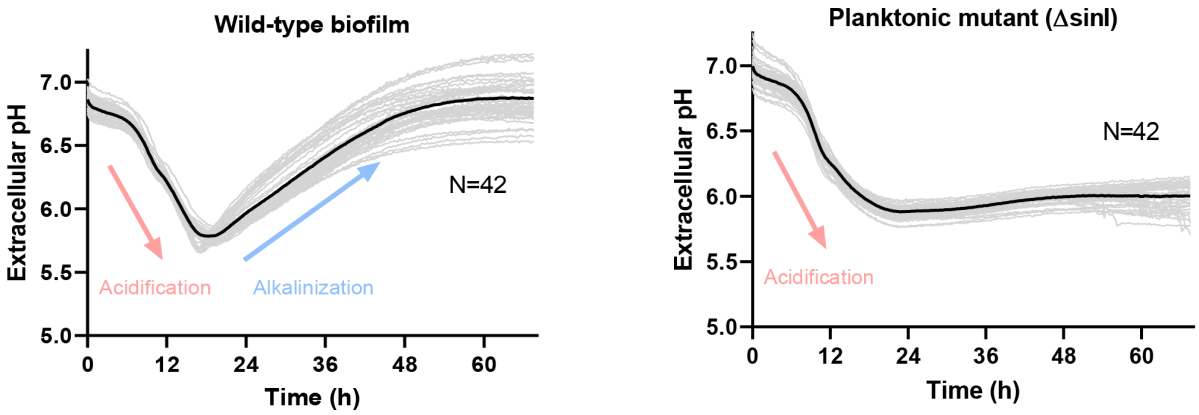


(a) (b)

**Figure 3.6.** Extracellular pH measurements for NCIB 3160 biofilms and planktonic cells. a, Extracellular pH measurements for NCIB 3610 WT biofilms. Data: mean ± std, n=42 technical replicates. Strain: NCIB 3610. b, Extracellular pH measurements for planktonic mutant NCIB 3610 ΔsinI. Data: mean ± std, n=42 technical replicates. Strain: NCIB 3610 ΔsinI.

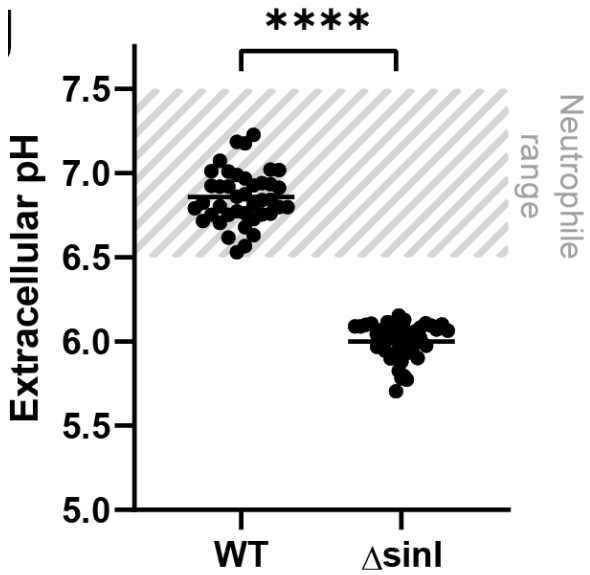


**Figure 3.7.** Comparison of extracellular pH between 3610 WT and ΔsinI after 60 h of growth. Biofilm end pH values were statistically higher compared to planktonic mutant ($p<0.05$). Data: n=42 technical replicates per strain. Statistical significance was calculated using a Students t-test with $p<0.000001$. Strains: NCIB 3610 and NCIB 3610 ΔsinI.

### 3.2.2. Genetic mechanisms responsible for extracellular pH modulation in biofilms

We sought to determine the genes responsible for driving the observed acidification and alkalinization. We considered metabolic pathways and processes that could both acidify and alkalinize the biofilm environment (Figure 3.8).

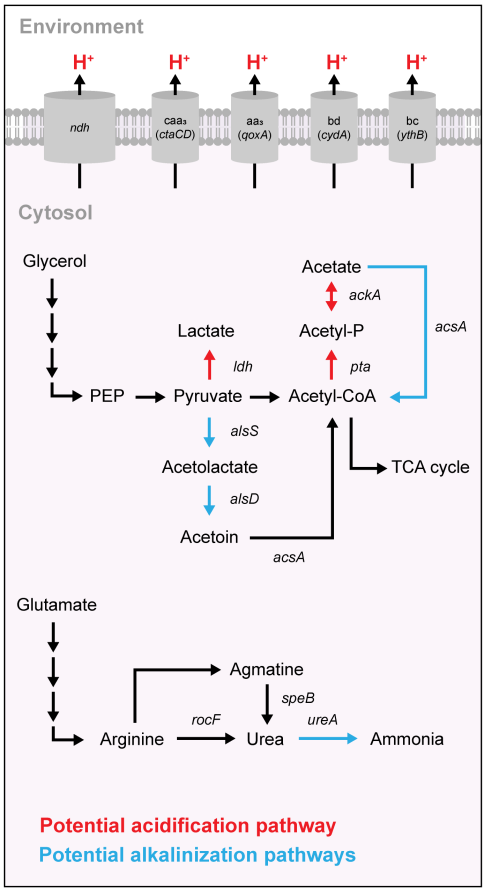


**Figure 3.8.** Schematic showing metabolic pathways in B. subtilis NCIB 3610 that are potential sources for extracellular acidification and alkalinization. Potential acidification pathways are highlighted in red whereas potential alkalinization pathways are highlighted in blue.

We first investigated ETC-associated complexes that can act as proton pumps and could drive acidification of the biofilm environment. We individually disrupted all 5 *B. subtilis* ETC complexes with known proton pump function and observed that no deletion produced significant change to the observed pH dynamic (Figure 3.9a). In the case of ΔctaCD, ΔqoxA, ΔcydA, and ΔythB mutants, each deletion was a major subunit in the ETC complex resulting in total loss of function for that enzyme. These results suggest that common sources of direct proton transport are not responsible for the observed pH dynamic.

We next suspected fermentation as a source of acidification since it is known that proliferating bacteria excrete acidic metabolites during overflow metabolism [**109**]. We initially suspected lactate fermentation, as lactate is commonly produced during exponential and stationary growth to replenish redox carriers [**126**]. Surprisingly, a lactate production-deficient mutant (Δldh) did not show any difference in acidification compared to WT (Figure 3.9b). We then considered acetate fermentation, where acetate production similarly yields ATP and provides a substrate for the TCA cycle (Figure 3.8). To determine if acetate fermentation is involved in biofilm pH regulation, we generated mutants for each enzyme in the acetate biosynthesis pathway. While an ackA mutant (ΔackA) retained the acidification phase (Figure 3.9c), a double mutant of ackA and acsA (ΔackAΔacsA), where acsA is an enzyme which can reversibly convert acetate into acetyl-CoA, had a reduced acidification phase. We quantified this reduction and observed that the ΔackAΔacsA mutant had an acidification rate approximately 48% less compared to wild type. Therefore, we concluded that acetate production is a primary source of acidification during biofilm development.

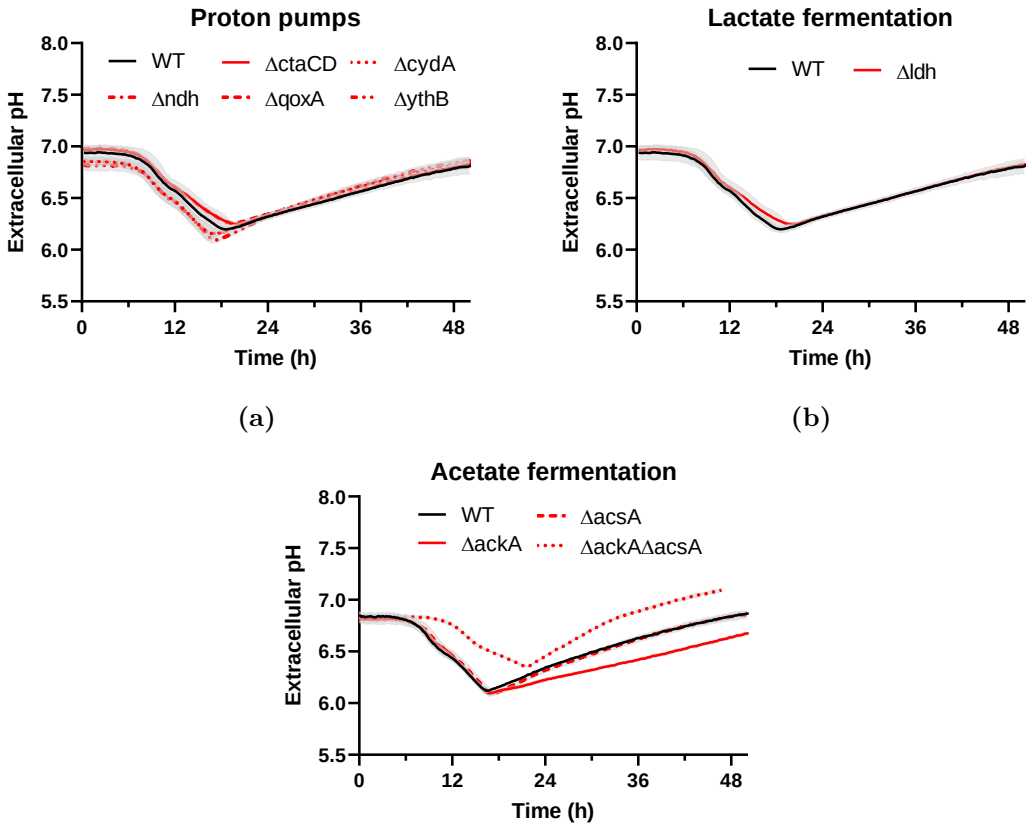


**Figure 3.9.** Potential pathways for extracellular acidification in biofilms. a, Extracellular pH measurements for proton pump mutants. Data: mean ± std, n=3 technical replicates. Strains: NCIB 3610, ΔctaCD, ΔcydA, Δndh, ΔqoxA, ΔythB. b, Extracellular pH measurements for lactate dehydrogenase mutant, Δldh. Data: mean ± std, n=3 technical replicates. Strains: NCIB 3610, Δldh. c, Extracellular pH measurements for acetate biosynthesis and catabolism mutants. Data: mean ± std, n=3 technical replicates. Strains: NCIB 3610, ΔackA, ΔackAΔacsA, ΔacsA.

On the other hand, to determine the genetic mechanism of alkalinization, we initially suspected ammonia as a critical community metabolite and known volatile alkaline species. However, deleting enzymes involved in ammonia synthesis produced no change to the alkalinization phase (Figure 3.10a). We then considered acetoin biosynthesis as a

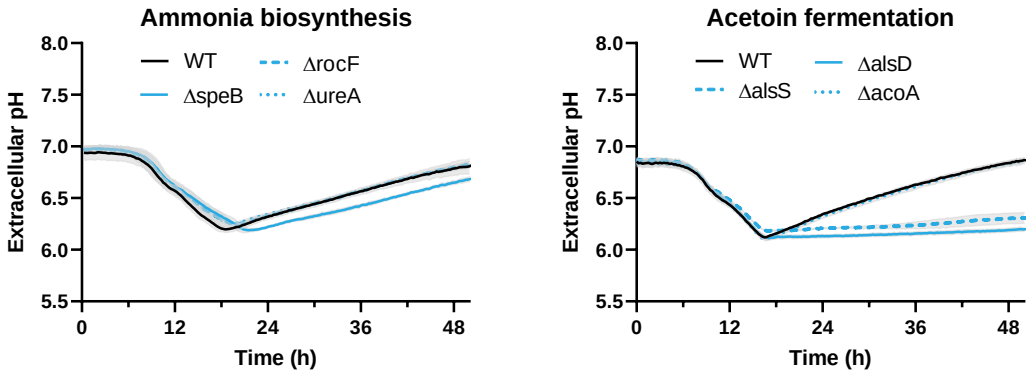


**(a)** **(b)**

**Figure 3.10.** Potential pathways for extracellular alkalinization in biofilms. a, Extracellular pH measurements for ammonia biosynthesis mutants. Data: mean ± std, n=3 technical replicates. Strains: NCIB 3610, ΔrocF, ΔspeB, ΔureA. b, Extracellular pH measurements for acetoin biosynthesis and catabolism mutants. Data: mean ± std, n=3 technical replicates. Strains: NCIB 3610, ΔalsS, ΔalsD. ΔacoaA.

pathway that has been speculated to circumvent lethal acidification via consumption of free protons [**127, 128, 129**]. The acetoin pathway consists of two enzymatic conversion steps where alsS (acetolactate synthase) converts pyruvate to acetolactate and alsD (acetoin synthase) converts acetolactate to acetoin, with each step consuming a proton (Figure 3.8). We generated mutants for each step and observed that both the alsS (ΔalsS) and alsD (ΔalsD) mutants retained the acidification phase yet completely lost the alkalinization phase (Figure 3.10b). We found that acetoin itself (up to 5 mM) produces no change in the magnitude nor timing of alkalinization (Figure 3.11). Therefore, we concluded that the acetoin biosynthesis process is responsible for alkalinization.

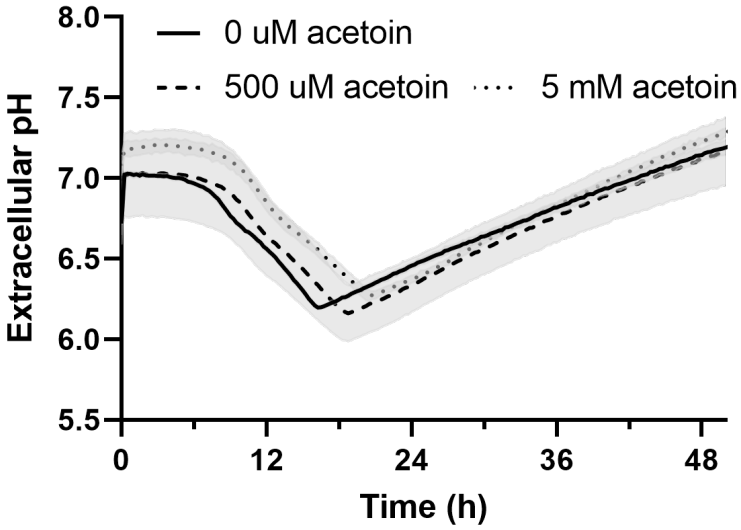


**Figure 3.11.** Extracellular pH measurements for biofilms grown in the presence of exogenous acetoin. Acetoin added to the starting minimally buffered MSgg with 10 uM BCECF at 0, 0.5, and 5 mM concentrations and inoculated with NCIB 3610 at 30°C. Biofilms were grown for approximately 50 h and BCECF. Data: mean ± std, n=3 technical replicates.

### 3.2.3. Active pH regulation during biofilm development via acetoin biosynthesis

We then asked whether biofilms could utilize acetoin biosynthesis as an active pH regulation mechanism. We grew biofilms in minimally buffered MSgg media conditioned to a range of initial pH values (pH 6 to 9) and tracked the local pH and alsS expression in each case (Figure 3.12).

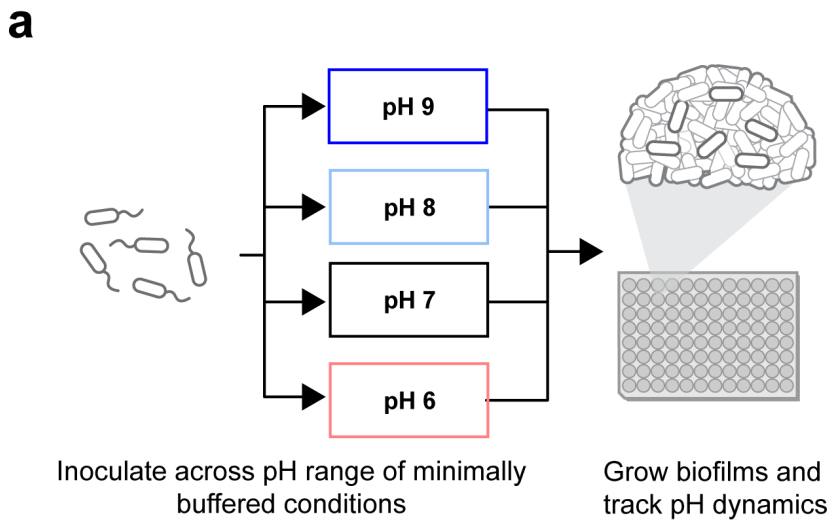


**Figure 3.12.** Schematic showing experimental workflow for growing biofilms across pH range and measuring extracellular pH dynamics during development.

Strikingly, we found that biofilms conditioned their local pH to the preferred neutrophile range by modulating both the magnitude and duration of the alkalinization phase (Figure 3.13a).

Specifically, in acidic initial conditions (pH 6) alkalinization proceeded at a rate of 0.03 pH/h over a longer duration (36.6 ± 0.4 h) compared to neutral initial conditions (31.2 ± 0.5 h) (Fig. 3c, d). Conversely, biofilms grown in basic conditions (pH 8 and 9)

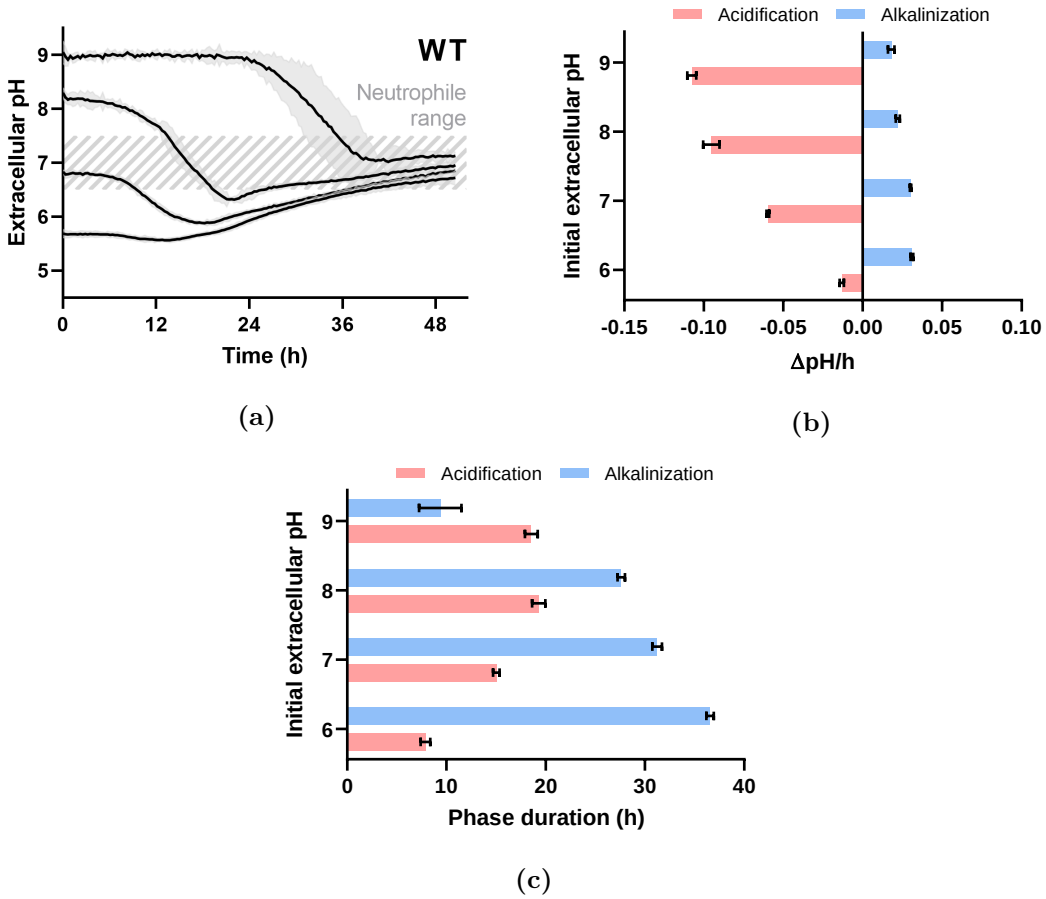


**Figure 3.13.** Characterization of biofilm extracellular pH dynamics during development. b, Measurement of extracellular pH for NCIB 3610 biofilms grown across a range of starting pH conditions (pH 6, 7, 8, 9). Dashed grey area represents optimal extracellular pH for neutrophile organisms. Biofilms were grown at 30°C statically. Data: mean ± std, n=3 technical replicates. c, Average acidification and alkalinization rates for biofilm extracellular pH. Data from ΔpH/h traces were analyzed and averaged to determine biofilm acidification (< 0 ΔpH/h) and alkalinization (> 0 ΔpH/h). Data: mean ± std, n=3 technical replicates. d, Phase duration for biofilm pH dynamics. Data from ΔpH/h traces were analyzed to determine biofilm acidification and alkalinization phase duration, by measuring time periods where ΔpH/h was predominately <0 and >0 respectively. Data: mean ± std, n=3 technical replicates.

minimized alkalinization in both magnitude and duration (Figures 3.13b, 3.13c). Interestingly, while the observed phases differed, biofilms grown at each pH condition produced

similar matrix levels as indicated by safranin staining (3.14). In agreement with these pH measurements, a PalsS-YFP reporter strain revealed that alsS expression was increased in acidic conditions and decreased in alkaline conditions (Figure 3.13c). Consequently, ΔalsS mutant biofilms failed to maintain their local pH in the preferred neutrophile range (Fig. 3e). Our data reveals that biofilms can use acetoin biosynthesis as an active pH regulation mechanism to mitigate growth-associated acidification even in non-ideal pH environments.

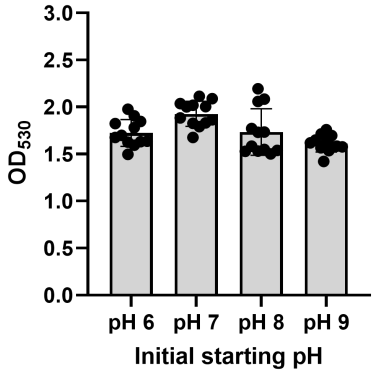


**Figure 3.14.** Safranin staining of biofilms grown at various pH starting conditions in minimally buffered MSgg. Biofilms were allowed to grow for approximately 68 h at 30Â°C. Biofilm matrix was isolated via aspiration of remaining media and air dried overnight at room temperature. Matrix was then stained with safranin solution for 10 min, washed three times with water, and allowed to dry for another 30 minutes. 30% acetic acid was added to the matrix and allowed to stain for 30 minutes before measuring final optical density of the stained matrix at 530 nm.

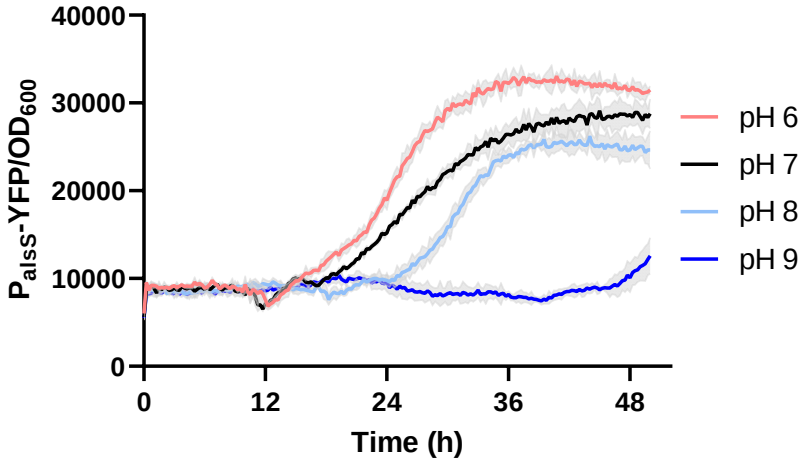


**Figure 3.15.** Measurements of acetoin biosynthesis via genetically encoded reporters for acetolactate synthase (alsS). Data: mean ± std, n=3 technical replicates. Strain: NCIB 3610

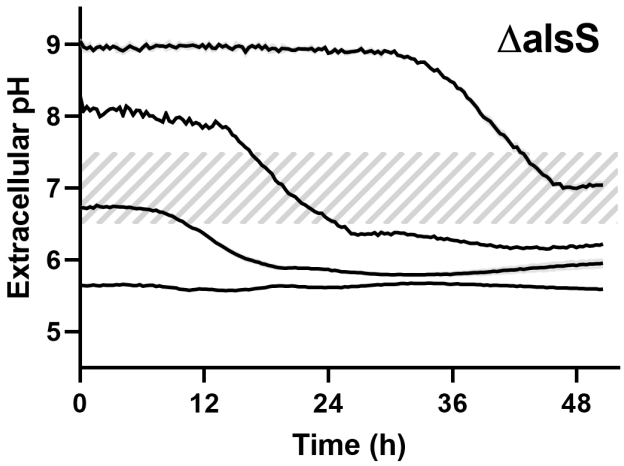


**Figure 3.16.** Measurement of extracellular pH for NCIB 3610 ΔalsS mutant biofilms grown across a range of starting pH conditions (pH 6, 7, 8, 9). Dashed grey area represents optimal extracellular pH for neutrophile organisms. Biofilms were grown at 30Â°C statically. Data: mean ± std, n=3 technical replicates.

To validate acetoin biosynthesis as an active pH regulation mechanism, we performed RNA sequencing (RNAseq) on WT and ΔalsS mutant biofilms to identify differentially expressed genes (DEGs) in both normal and minimally buffered media. We confirmed that the alsSD pathway was upregulated in WT biofilms in minimally buffered media (Fig. 3f). Interestingly, we found that ΔalsS mutant biofilms grown in minimally buffered media upregulated ilvBH, an alternate acetolactate synthase that could potentially compensate for loss of alsS activity (Figure 3.17). We confirmed that ΔilvBH mutant biofilms also showed reduced alkalization, but with an added growth defect due to the role of ilvBH in branched-chain amino acids biosynthesis (Supplemental Fig. 5). As expected, we observed upregulation of several acid stress genes in ΔalsS mutant biofilms grown in minimally buffered media (Figure 3.18). In addition, we observed upregulation of several oxidative stress genes in ΔalsS mutant biofilms (Figure 3.18). This oxidative stress may result from a dysregulation of the PMF when active pH regulation is absent. Taken together, these results confirm that biofilms utilize acetoin biosynthesis as a form of active pH regulation to maintain pH homeostasis and minimize cellular stress.

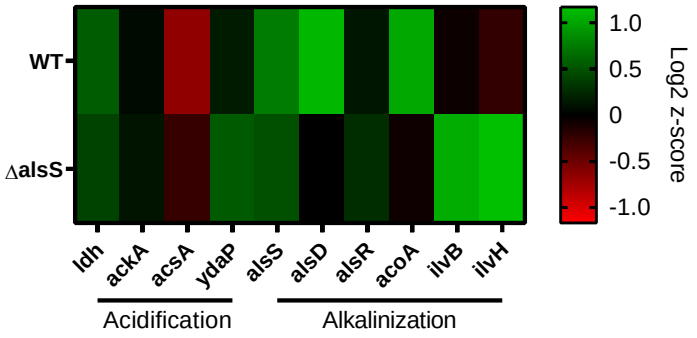


**Figure 3.17.** Heat map showing differentially expressed genes in overflow metabolism and potential candidates for extracellular acidification and alkalinization, induced by minimization of extracellular buffer, n=3.

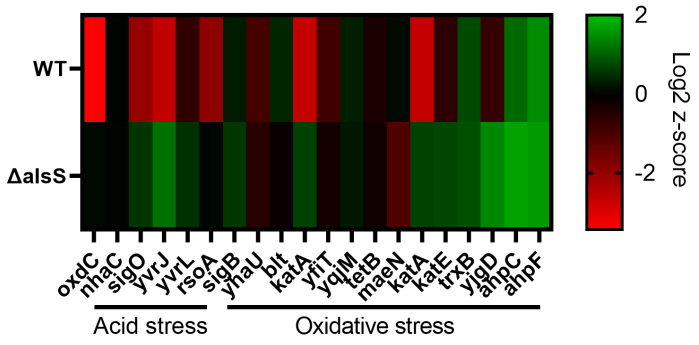


**Figure 3.18.** Heat map showing differentially expressed genes in acid and oxidative stress, induced by minimization of extracellular buffer, n=3.

### 3.2.4. Physiological characterization of B. subtilis biofilms and buffering-deficient mutants

Accordingly, we wondered if active pH regulation could facilitate biofilm development in minimally buffered conditions. We first compared WT and ΔalsS biofilms on buffered media and found no significant difference in their overall growth and morphology (Figure 3.19a, top). However, while WT biofilms largely maintained biofilm morphology in minimally buffered conditions, ΔalsS mutant biofilms lacked macroscopic wrinkles and displayed altered biofilm morphology, suggesting a difference in the biofilm ECM that maintains biofilm structure (Figure 3.19a, bottom). In agreement with these observations, we found that ΔalsS biofilms had a significantly lower cell count ($p<0.001$) that was specific to minimally buffered conditions, suggesting that inability to alkalinize via acetoin production was detrimental to biofilm growth (Figure 3.19b). These results suggest that acetoin biosynthesis plays a role in biofilm development specific to minimally buffered environments.

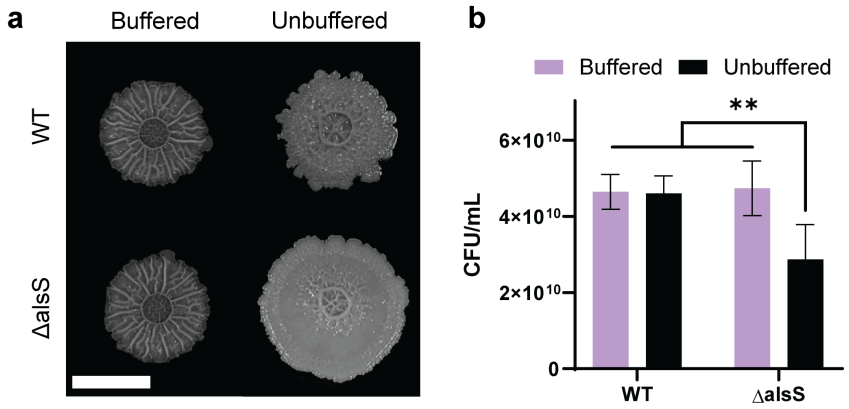


**Figure 3.19.** Microscopy and cell density quantification for NCIB 3610 WT and ΔalsS biofilms grown on buffered and minimally buffered conditions. a, Images of B. subtilis NCIB 3610 WT and ΔalsS on buffered and minimally buffered MSgg solid agar, grown over 60 h. Scale bar represents 2 mm. b, CFU measurements of 3610 WT and ΔalsS biofilms grown on buffered and minimally buffered MSgg solid agar harvested at 60 h. Data: mean ± std, n=6 technical replicates.

To corroborate these findings, we performed RNAseq analysis to identify DEGs associated with biofilm development and extracellular matrix (ECM) production. We found that ΔalsS mutant biofilms grown in minimally buffered media downregulated 16 of the 18 known ECM-associated genes in *B. subtilis* while WT biofilms did not (Figure 3.20).

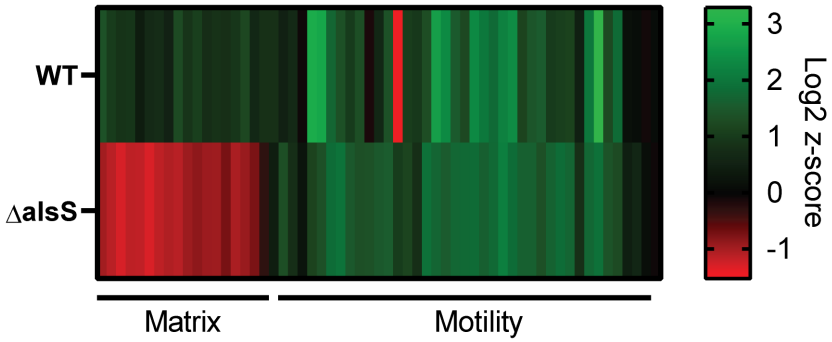


**Figure 3.20.** Heat map showing differentially expressed genes associated with matrix and motility in NCIB 3610 WT and ΔalsS biofilms, induced by minimization of extracellular buffer, n=3.

We then created a genetically encoded fluorescent reporter for tapA, the anchoring and assembly protein for biofilm amyloid fiber. As expected, we found that WT biofilms displayed comparable tapA reporter expression in both buffered and minimally buffered conditions, in agreement with our prior observations on biofilm morphology (Figure 3.21d, left). In contrast, while ΔalsS biofilms had comparable tapA reporter expression in buffered conditions, we measured significantly reduced ($p<0.0001$) tapA expression in minimally buffered conditions (Figures 3.21d, right, 3.21e). Interestingly, both ΔalsS mutant biofilms and WT biofilms upregulated motility genes in minimally buffered conditions, suggesting that active pH regulation via acetoin biosynthesis may serve to prevent acidification-associated biofilm dispersal. Taken together, these results confirm that active pH regulation facilitates biofilm ECM formation in minimally buffered conditions.

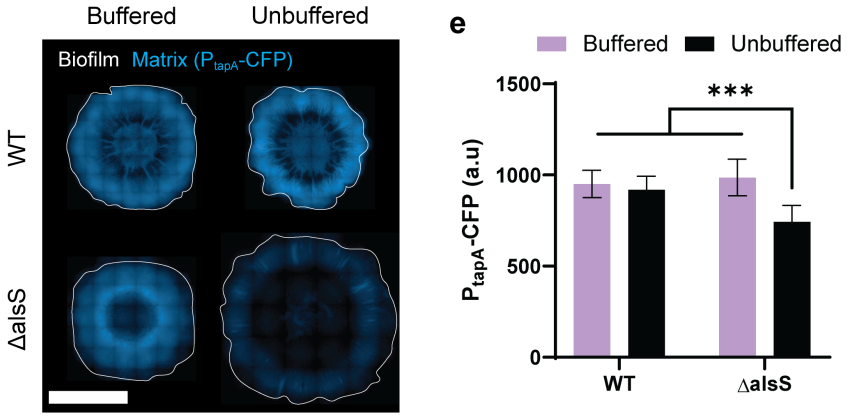


**Figure 3.21.** Microscopy and quantification of tapA matrix protein expression in NCIB 3610 WT and ΔalsS biofilms, induced by minimization of extracellular buffer. a, Fluorescence microscopy images of 3610 WT and ΔalsS biofilms expressing PtapA-CFP on buffered and minimally buffered MSgg solid agar at 36 h. White outline denotes biofilm edge, blue represents tapA matrix expression. Scale bar represents 2 mm. b, Fluorescence measurements of 3610 WT and ΔalsS biofilms grown on buffered and minimally buffered MSgg solid agar harvested at 36 h. Data: mean ± std, n=6 technical replicates.

We then asked how active pH regulation impacts biofilm resilience to antibiotic treatment since previous studies have shown that biofilms can possess more antibiotic tolerance compared to planktonic cells [**12, 19**]. To test this, we grew WT and ΔalsS mutant biofilms in minimally buffered media and exposed the biofilms to antibiotic treatment. We chose a panel of antibiotics consisting of kanamycin, tetracyline, streptomycin, and neomycin, as well as water as a vehicle. We found that ΔalsS mutant biofilms were more sensitive to kanamycin (16%) and tetracycline (13%) treatment compared to WT biofilms (Figure 3.16). We also observed a lesser sensitivity to neomycin (7%) and streptomycin (11%). While disruption of acetoin biosynthesis did not completely sensitize biofilms to antibiotic treatment, these results suggest that active pH regulation allows biofilms to grow and produce ECM in tandem to better tolerate such exposures.

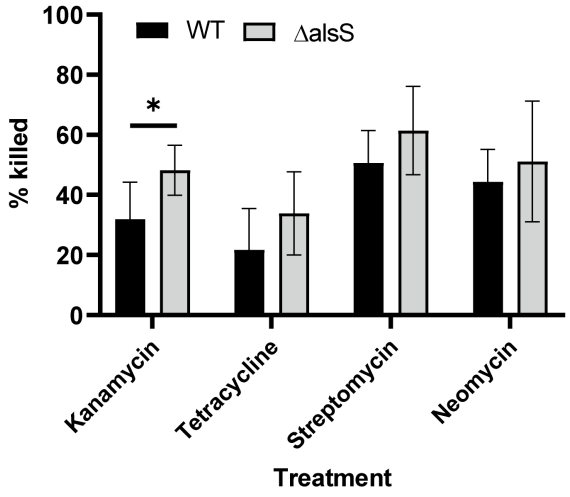


**Figure 3.22.** Antibiotic treatment efficacy (% killed), as measured by CFUs of harvested biofilms exposed to antibiotic (approximately 1700x MIC values reported for B. subtilis). % killed metric was calculated by comparing CFU of viable biofilm cells post 2 h treatment exposure vs. viable cells after exposure to water vehicle. Data: mean ± std, n=8 technical replicates across two experiments. Statistical significance was calculated using a Students t-test with * representing p¡0.05. Strain: NCIB 3610, ΔalsS.

## 3.3. Discussion

In our study, we established a minimally buffered system to determine how undomesticated *B. subtilis* biofilms cope with growth-associated acidification. We discovered an active pH regulation mechanism that effectively mitigates both growth-associated acidification and external pH challenges. This phenomenon is fully masked in buffered laboratory media and relies on the pH-dependent expression of acetoin biosynthesis. Disruption of acetoin biosynthesis results in dysregulated biofilm development, decreased extracellular matrix production, and increased antibiotic sensitivity. Thus, this active pH regulation mechanism enables biofilms to minimize cellular stresses and maintain community resilience against both internal growth-associated acidification and external pH challenges (Figure 3.23).

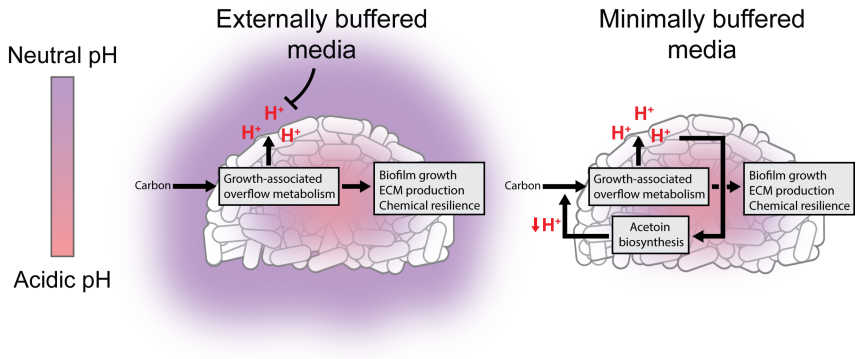


**Figure 3.23.** Proposed schematic of active pH regulation in biofilms.

Additional studies will be needed to determine whether this active pH regulation mechanism is found in other biofilm-forming species. While acetoin biosynthesis is largely conserved across both Gram-positive and Gram-negative bacteria, the pH-dependent expression of these pathways, especially in minimally buffered conditions, remains an open

question. Furthermore, while overflow metabolism has been well characterized in planktonic lab strains of Escherichia coli, its potential impact on biofilm development and pH regulation remains unclear [**109, 130**]. We propose that overflow metabolism, and specifically acetoin biosynthesis, provides a critical detoxification pathway for immobilized and densely packed communities during biofilm development. Our proposal aligns with and extends mechanistic single-cell level studies that reveal the potential role of acetoin biosynthesis in mitigating local acidification [**22**]. Future studies may also elucidate how active pH regulation influences other emergent behaviors observed in biofilms. For example, in natural environments such as soil, geothermal springs, and human gastrointestinal tract, variations and gradients in pH give rise to unique bacterial behaviors such as extracellular electron transport, chemotropy, and increased drug resistance [**131, 132, 133**]. Our results are also intriguing to consider alongside recent results which show acetate biosynthesis pathway promoting biofilm development over macroscopic length scales [**134, 135**]. As biofilm growth appears to necessitate acetate production, it would be interesting to determine how local acetate production influences nearby communities, and how each community integrates their local needs with those of their neighbors. Active pH regulation could also help stabilize the PMF of biofilm cells during electrochemical signaling, enabling cells to modulate ionic efflux and membrane voltage while maintaining cellular growth. In summary, while chemical buffers are often employed to study biofilms in the laboratory, they also mask the underlying biology of pH management during biofilm development. pH is one of the most fundamental forces shaping chemical biology across all domains of life. From bacteria to cancer, rapid cellular proliferation demands the use of overflow metabolism which can often result in excessive acidification. However, in

the case of bacterial communities known as biofilms, the underlying biological interplay between growth and pH has been largely masked due to the use of buffered laboratory media in biofilm studies. The discovery of active pH regulation in biofilms could provide new opportunities for understanding microbial communities, controlling pathogenic biofilm growth, and engineering novel biofilm behaviors.

## 3.4. Methods

### 3.4.1. Strains

| Strain | Organism | Genotype |
|---|---|---|
| Wild type | *B. subtilis* NCIB 3610 | |
| Δ*sinI* | *B. subtilis* NCIB 3610 | *sinI*::neo |
| Δ*ndh* | *B. subtilis* NCIB 3610 | *ndh*::kan |
| Δ*ctaCD* | *B. subtilis* NCIB 3610 | *ctaCD*::neo |
| Δ*cydA* | *B. subtilis* NCIB 3610 | *cydA*::neo |
| Δ*qoxA* | *B. subtilis* NCIB 3610 | *qoxA*::neo |
| Δ*ythB* | *B. subtilis* NCIB 3610 | *ythB*::neo |
| Δ*ldh* | *B. subtilis* NCIB 3610 | *ldh*::kan |
| Δ*ackA* | *B. subtilis* NCIB 3610 | *ackA*::kan |
| Δ*acsA* | *B. subtilis* NCIB 3610 | *acsA*::kan |
| Δ*ackA*Δ*acsA* | *B. subtilis* NCIB 3610 | *ackA*::acsA::kan |
| Δ*rocF* | *B. subtilis* NCIB 3610 | *rocF*::kan |
| Δ*speB* | *B. subtilis* NCIB 3610 | *speB*::kan |
| Δ*ureA* | *B. subtilis* NCIB 3610 | *ureA*::kan |
| Δ*alsS* | *B. subtilis* NCIB 3610 | *alsS*::kan |
| Δ*alsD* | *B. subtilis* NCIB 3610 | *alsD*::kan |
| Δ*acoA* | *B. subtilis* NCIB 3610 | *acoA*::kan |
| $P_{alsS}$-YFP | *B. subtilis* NCIB 3610 | *sacA*::$P_{alsS}$-YFP::cm |
| $P_{hag}$-mCherry, $P_{tapA}$-CFP | *B. subtilis* NCIB 3610 | *amyE*::$P_{hag}$-mCherry::mls, *sacA*::$P_{tapA}$-CFP::cm |
| Δ*alsS* $P_{hag}$-mCherry, $P_{tapA}$-CFP | *B. subtilis* NCIB 3610 | *amyE*::$P_{hag}$-mCherry::mls, *sacA*::$P_{tapA}$-CFP::cm |

### 3.4.2. Growth conditions

Bacteria were grown in Luria-Bertani (LB) rich media overnight and or grown day-of experiment and seeded into MSgg media. Biofilms in fully buffered conditions were grown in standard MSgg, which contains 100 mM MOPS, 5 mM potassium-phosphate buffer (pH 7), 2 mM MgCl2, 700 $\mu$M CaCl2, 50 $\mu$M MnCl2, 100 $\mu$M FeCl3, 1 $\mu$M ZnCl2, 2 $\mu$M thiamine HCl, 0.5% (v/v) glycerol, and 0.5% (w/v) monosodium glutamate. Biofilms in minimally buffered conditions were grown in modified MSgg, which contains 1 mM MOPS, 5 mM potassium-phosphate buffer (pH 7), 2 mM MgCl2, 700 $\mu$M CaCl2, 50 $\mu$M MnCl2, 100 $\mu$M FeCl3, 1 $\mu$M ZnCl2, 2 $\mu$M thiamine HCl, 0.5% (v/v) glycerol, and 0.5% (w/v) monosodium glutamate. To measure biofilm extracellular pH, 10 $\mu$M BCECF free acid (Biotium) was used in MSgg. Strains were grown to OD 0.8-1.0 in LB, spun down and resuspended in 1x PBS. 1 $\mu$L cell culture was then seeded into 199 $\mu$L MSgg in a 96-well microplate (Corning 3904) or into a well with 0.6 mL solid MSgg agar in a 24-well plate (Corning 3526).

### 3.4.3. Optical density, fluorescence, and cell density measurements

Optical density (530 and 600 nm), BCECF, and YFP fluorescence in all our studies were measured using a TECAN Infinite MPLEX plate reader with excitation/emission wavelength set to 503/530 nm and gain set to 100. To quantify biofilm extracellular pH, minimally buffered MSgg was prepared for each experiment and conditioned to pH 5, 6, 7, 8, and 9 using 1 M HCl and 1 M NaOH when appropriate. BCECF dye was then added to these aliquots and included as a standard curve to convert the measured BCECF fluorescence signal to extracellular pH. Cell density of biofilms or planktonic cultures were

quantified using a hemocytometer or Logos Biosystems Quantom TX Microbial Counter. To prepare biofilms for cell density quantification, biofilms were grown for the desired time in either buffered or minimally buffered MSgg media. Each biofilm was harvested into 1 mL 1x PBS solution and sonicated for 5 s on ice using a Qsonica Q125 125W 20 kHz sonicator at 60% amplitude. For hemocytometer counting, the resulting cell suspension was fixed with paraformaldehyde, diluted into PBS, and counted using phase microscopy. For the Quantom TX, the cell suspension was diluted into PBS and stained using the Logos Total Cell Staining kit and imaged directly on the Quantom TX.

### 3.4.4. DNA cloning

Custom promoter sequences were ordered from Integrated DNA Technologies (IDT) or amplified from the native NCIB genome and cloned upstream of YFP reporter in a B. subtilis integration vector ECE174 (https://bgsc.org/search.php?Search=ece174) with chloramphenicol resistance. All plasmid assembly was performed using Gibson Assembly using the Gibson Assembly Master Mix (NEB). The assembled plasmid was transformed into NCIB 3610 using a natural competence protocol previously described and plated on LB agar with appropriate selection [**136**].

### 3.4.5. RNA isolation

3610 biofilms were grown for 36 h in either buffered or minimally buffered MSgg media. Each biofilm was harvested into 1 mL 1x PBS solution and sonicated for 5 s on ice using a Qsonica Q125 125W 20 kHz sonicator at 60% amplitude. RNA was then isolated using the QIAGEN RNeasy kit (QIAGEN) according to manufacturer's instructions.

### 3.4.6. RNA-sequencing

RNA quality was checked using Bioanalyzer (Agilent) prior to RNA-seq library preparation. RNA samples with an RNA integrity number >8 were used for library preparation, which was constructed from 100 ng of RNA with the Illumina Stranded Total RNA Prep, Ligation with Ribo-Zero Plus kit (Illumina). RNA Sequencing was then performed on NovaSeq 6000 sequencer and analyzed as previously described. The quality of reads, in FASTQ format, was evaluated using FastQC. Reads were trimmed to remove Illumina adapters from the 3' ends using cutadapt (Martin, 2011). Trimmed reads were aligned to the Bacillus subtilis genome strain 3610 NCBI CP020102.1 and plasmid NCBI CP020103.1 using STAR (Dobin et al, 2013). Read counts for each gene were calculated using htseq-count (Anders et al, 2015) in conjunction with a gene annotation file for the reference genomes obtained from NCBI. Normalization and differential expression were calculated using DESeq2 that employs the Wald test (Love et al, 2014). The cutoff for determining significantly differentially expressed genes was an FDR-adjusted p-value less than 0.05 using the Benjamini-Hochberg method.

### 3.4.7. Microscopy

Biofilm growth was recorded using phase contrast and fluorescence microscopy. The microscope used was a Nikon Ti2. To image entire biofilms, we used 10x objective and the stitching function in Nikon Elements to assemble images. Images were taken every hour. Whenever fluorescence images were recorded, we used the minimum exposure time that still provided a good signal-to-noise ratio.

### 3.4.8. Image analysis

Fiji/ImageJ (National Institutes of Health) was used for image analysis. To measure biofilm fluorescence, we identified the biofilm area first using phase and creating custom regions of interests (ROIs) that outlined the biofilm for each frame. We then used the same ROIs on the relevant fluorescent channel of the same experimental run to measure average fluorescent reporter signal over time.

### 3.4.9. Treatment of biofilms with antibiotics

We grew biofilms on minimally buffered MSgg agar for 48 h, harvested the intact biofilms, and submerged them into 1 mL of treatment solution for 2 h, where the antibiotic concentration was approximately 1700 times higher than the reported MIC values for B. subtilis.50 Treatment concentrations for kanamycin and tetracycline were 12.8 mg per mL water. Treatment concentrations for streptomycin and neomycin were 17 and 10 mg/mL water respectively. After exposure we washed the biofilms twice with saline solution (9 g NaCl per liter ddH2O) and sonicated the biofilm solution for 5 s on ice using a Qsonica Q125 125W 20 kHz sonicator at 60% amplitude. The resulting cell dispersion was serially diluted into saline solution and plated on LB to count to quantify viable biofilms cells after treatment.

### 3.4.10. Statistical analyses

Statistical tests were calculated in GraphPad Prism 9.0. For comparisons between two independent groups, a Student's T-test was used. Significance was accepted at $p<0.05$. The details of the statistical tests carried out are indicated in respective figure legends.

CHAPTER 4

# Conclusion

Bacteria represent the most abundant form of life on Earth and can colonize nearly every environmental niche. In these environments, bacteria predominately form multicellular communities known as biofilms where bacteria engage in complex social behaviors and gain new collective properties (e.g. increased persistence and resilience). Due to such ubiquity and emergent behaviors, biofilms present an attractive target for engineering and synthetic biology. Importantly, understanding biofilm physiology can elucidate mechanisms enabling pathogenic biofilms and provide new modalities for multicellular control. While biofilms provide individual bacteria many advantages, there still remains significant need to discover and characterize the processes within biofilms that enable their behaviors. Furthermore, the dense cellular proliferation associated with biofilm development also creates intrinsic metabolic challenges including excessive acidification associated with overflow metabolism. Because such pH stress is commonly masked in buffered laboratory media, it remains unclear how biofilms cope with minimally buffered natural environments.

This dissertation addresses these needs with development of new methods to interrogate biofilm physiology and behavior *in situ* with a focus on biofilm energy metabolism and pH regulation.

The first contribution of this dissertation is the method development for *in situ* measurement of biofilm energy metabolism using metabolic flux analysis. The Agilent Seahorse Xe96 platform has previously been used to study energy metabolism flux in both eukaryotic and planktonic bacterial cells, and here we adapt this technology to study biofilm respiration over the course of biofilm development and maturation. This dissertation shows that *B. subtilis* biofilms can be 1) cultured in the Seahorse system and 2) show distinct respiration differences compared to both planktonic and domesticated strains. In doing so, we can now further track how bacteria metabolically remodel as they transition from the planktonic state to biofilm. Additionally, this methods allows the study of multiple strains at once per experiment, along with the ability to expose biofilms to different environmental challenges including pH and drug treatment. This method has also revealed that biofilm metabolically react to antibiotic treatment distinctly different compared to planktonic cells. Overall, this provides a robust platform to study biofilm energy metabolism with relatively high-throughput under many different environmental conditions.

The second contribution of this dissertation is the discovery and characterization of active pH regulation in biofilms under minimally buffered conditions. Previous biofilm studies have been performed in fully buffered conditions, where external chemical buffer in the culture media can mask underlying pH dynamics in biofilms. Work in this dissertation has shown that biofilms can 1) tolerate minimally buffered conditions without any significant effect on growth, 2) actively regulate their extracellular pH during biofilm development to maintain neutral pH and 3) such pH regulation supports biofilm matrix development and resilience against antibiotic treatment. Overall, this work reveals active

pH regulation as an emergent behavior in bacterial biofilms that be targeted for future studies to control biofilm growth.

This dissertation provides new tools to study bacterial biofilms and specifically their pH dynamics. In doing so, this contributes to our further understanding of biofilms and will enable future work on controlling and engineering biofilms.

## 4.1. Future work

Based on the work presented in this dissertation, future efforts can expand in several directions: 1) improving *in situ* measurement of biofilm energy metabolism, 2) further characterizing active pH regulation in biofilms, and 3) engineering pH-stabilizing biofilms.

### 4.1.1. Improving *in situ* measurement of biofilm energy metabolism

Future work will involve determining the mechanisms by which bacterial biofilm communities co-regulate their energy metabolic processes to evade these effects of antibiotics. For example, it is possible that disrupting biofilm-specific acidification may provide a means to render biofilms more susceptible to antibiotics. In this context, the high-throughput nature of our method is compatible both with genetic studies using deletion libraries as well as chemical small molecule screens. Our method will enhance basic microbiology studies toward understanding the emergent metabolic behaviors of the most pervasive bacterial lifestyle, while also accelerating biomedical research to combat antibiotic resistant biofilm-mediated infections.

### 4.1.2. Characterizing active pH regulation in biofilms

Future work will be needed to determine whether active pH regulation mechanism is found in other biofilm-forming species. While acetoin biosynthesis is largely conserved across both Gram-positive and Gram-negative bacteria, the pH-dependent expression of these pathways, especially in minimally buffered conditions, remains an open question. Furthermore, while overflow metabolism has been well characterized in planktonic lab strains of Escherichia coli, its potential impact on biofilm development and pH regulation remains unclear [**109, 130**]. We propose that overflow metabolism, and specifically acetoin biosynthesis, provides a critical detoxification pathway for immobilized and densely packed communities during biofilm development. Our proposal aligns with and extends mechanistic single-cell level studies that reveal the potential role of acetoin biosynthesis in mitigating local acidification [**22**]. Future studies may also elucidate how active pH regulation influences other emergent behaviors observed in biofilms. For example, in natural environments such as soil, geothermal springs, and human gastrointestinal tract, variations and gradients in pH give rise to unique bacterial behaviors such as extracellular electron transport, chemotropy, and increased drug resistance [**131, 132, 133**]. Our results are also intriguing to consider alongside recent results which show acetate biosynthesis pathway promoting biofilm development over macroscopic length scales [**134, 135**]. As biofilm growth appears to necessitate acetate production, it would be interesting to determine how local acetate production influences nearby communities, and how each community integrates their local needs with those of their neighbors. Active pH regulation could also help stabilize the PMF of biofilm cells during electrochemical signaling,

enabling cells to modulate ionic efflux and membrane voltage while maintaining cellular growth.

### 4.1.3. Engineering pH-stabilizing biofilms

Opportunity remains to co-opt the complex social behaviors of biofilms (e.g. cell-to-cell signaling, division of labor, and matrix production) for medicine, biomanufacturing, and environmental remediation. Additionally, basic scientific study of these processes could provide inspiration for more sophisticated synthetic gene circuits beyond the biofilm context, especially with relation to pH regulation. In addition to intercellular coordination, the physical robustness and environmental persistence of biofilms could enable new living materials and robust deployment of engineered bacteria into target environments. Indeed, future efforts can be directed towards engineering biofilms with pH-regulating circuits such that biofilms can maintain their preferred local extracellular pH even in heterogeneous and non-ideal conditions. These advances may also prove valuable beyond synthetic biology, impacting fields spanning materials science, ecology, and medicine. Overall, engineering individual bacteria has been instrumental to the advancement of synthetic biology thus far and the field is now poised to leverage bacterial biofilms for next generation synthetic biology applications

CHAPTER 5

# Publications

The following list presents publications with work from this dissertation in chronological order.

(1) Schofield Z, Meloni GN, **Tran P**, et al. Bioelectrical understanding and engineering of cell biology. *J R Soc Interface*. 2020;17(166). doi:10.1098/rsif.2020.0013

(2) **Tran P**, Prindle A. Synthetic biology in biofilms: Tools, challenges, and opportunities. *Biotechnol Prog*. 2021;37(5). doi:10.1002/btpr.3123

(3) Quillin SJ, **Tran P**, Prindle A. Potential Roles for Gamma-Aminobutyric Acid Signaling in Bacterial Communities. *Bioelectricity*. 2021;3(2):120-125. doi:10.1089/bioe.2021.0012

(4) Everett BA, **Tran P**, Prindle A. Toward manipulating serotonin signaling via the microbiota-gut-brain axis. *Curr Opin Biotechnol*. 2022;78. doi:10.1016/j.copbio.2022.102826

(5) Xia J, Hepler C, **Tran P**, Waldeck N, Li T, Bass J, Prindle A. Engineered calprotectin sensing probiotics for IBD surveillance in humans. *Proc Natl Acad Sci*. 2023 Accepted.

(6) **Tran P**, Prindle A. Active pH regulation facilitates biofilm development in minimally buffered environments. 2023 Submitted.

# References

[1] Hans Curt Flemming, Jost Wingender, Ulrich Szewzyk, Peter Steinberg, Scott A. Rice, and Staffan Kjelleberg. Biofilms: An emergent form of bacterial life. *Nature Reviews Microbiology*, 14:563–575, 2016.

[2] Hans Curt Flemming and Stefan Wuertz. Bacteria and archaea on earth and their abundance in biofilms. *Nature Reviews Microbiology*, 17:247–260, 2019.

[3] Anna Dragoš and Ákos T. Kovács. The peculiar functions of the bacterial extracellular matrix. *Trends in Microbiology*, 25:257–266, 2017.

[4] Hans-Curt Flemming and Jost Wingender. The biofilm matrix. *Nature Reviews Microbiology*, 8:623–633, 2010.

[5] Arthur Prindle, Jintao Liu, Munehiro Asally, San Ly, Jordi Garcia-Ojalvo, and Gürol M. Süel. Ion channels enable electrical communication in bacterial communities. *Nature*, 527:59–63, 2015.

[6] Joseph W. Larkin, Xiaoling Zhai, Kaito Kikuchi, Samuel E. Redford, Arthur Prindle, Jintao Liu, Sacha Greenfield, Aleksandra M. Walczak, Jordi Garcia-Ojalvo, Andrew Mugler, and Gürol M. Süel. Signal percolation within a bacterial community. *Cell Systems*, 7:137–145.e3, 8 2018.

[7] Nan Luo, Shangying Wang, Jia Lu, Xiaoyi Ouyang, and Lingchong You. Collective colony growth is optimized by branching pattern formation in pseudomonas aeruginosa. *Molecular Systems Biology*, 17, 4 2021.

[8] Liyang Xiong, Yuansheng Cao, Robert Cooper, Wouter Jan Rappel, Jeff Hasty, and Lev Tsimring. Flower-like patterns in multi-species bacterial colonies. *eLife*, 9, 1 2020.

[9] Andrew E. Blanchard and Ting Lu. Bacterial social interactions drive the emergence of differential spatial colony structures. *BMC Systems Biology*, 9, 9 2015.

[10] George O'Toole, Heidi B. Kaplan, and Roberto Kolter. Biofilm formation as microbial development. *Annual Review of Microbiology*, 54:49–79, 10 2000. doi: 10.1146/annurev.micro.54.1.49.

[11] Tippapha Pisithkul, Jeremy W. Schroeder, Edna A. Trujillo, Ponlkrit Yeesin, David M. Stevenson, Tai Chaiamarit, Joshua J. Coon, Jue D. Wang, and Daniel Amador-Noguez. Metabolic remodeling during biofilm development of bacillus subtilis. *mBio*, 10:e00623–19, 6 2019.

[12] Niels Høiby, Thomas Bjarnsholt, Michael Givskov, Søren Molin, and Oana Ciofu. Antibiotic resistance of bacterial biofilms. *International journal of antimicrobial agents*, 35:322–332, 4 2010.

[13] Anahit Penesyan, Ian T Paulsen, Staffan Kjelleberg, and Michael R Gillings. Three faces of biofilms: a microbial lifestyle, a nascent multicellular organism, and an incubator for diversity. *npj Biofilms and Microbiomes*, 7:80, 2021.

[14] Razan N. Alnahhas and Mary J. Dunlop. Advances in linking single-cell bacterial stress response to population-level survival. *Current Opinion in Biotechnology*, 79, 2 2023.

[15] Y. Chen, J. K. Kim, A. J. Hirning, K. Josi, and M. R. Bennett. Emergent genetic oscillations in a synthetic microbial consortium. *Science*, 349:986–989, 2015.

[16] J A Cole, L Kohler, J Hedhli, and Z Luthey-Schulten. Spatially-resolved metabolic cooperativity within dense bacterial colonies. *BMC Syst Biol*, 9:15, 2015.

[17] L Hall-Stoodley, J W Costerton, and P Stoodley. Bacterial biofilms: from the natural environment to infectious diseases. *Nat Rev Microbiol*, 2:95–108, 2004.

[18] Mary Ellen Davey and George A O'toole. Microbial biofilms: from ecology to molecular genetics. *Microbiology and Molecular Biology Reviews*, 64:847–867, 2000.

[19] Philip S Stewart and J William Costerton. Antibiotic resistance of bacteria in biofilms. *The Lancet*, 358:135–138, 2001.

[20] Elizabeth A Libby and Pamela A Silver. Harnessing undomesticated life. *Nature Microbiology*, 4:212–213, 2019.

[21] V. de Lorenzo. Recombinant bacteria for environmental release: What went wrong and what we have learnt from it. *Clinical Microbiology and Infection*, 15:63–65, 2009.

[22] Adam Z Rosenthal, Yutao Qi, Sahand Hormoz, Jin Park, Sophia Hsin-Jung Li, and Michael B Elowitz. Metabolic interactions between dynamic bacterial subpopulations. *eLife*, 7:e33099, 2018.

[23] Anna Dragoš, Heiko Kiesewalter, Marivic Martin, Chih Yu Hsu, Raimo Hartmann, Tobias Wechsler, Carsten Eriksen, Susanne Brix, Knut Drescher, Nicola Stanley-Wall, Rolf Kümmerli, and Ákos T. Kovács. Division of labor during biofilm matrix production. *Current Biology*, 28:1903–1913.e5, 2018.

[24] Jintao Liu, Arthur Prindle, Jacqueline Humphries, Marçal Gabalda-Sagarra, Munehiro Asally, Dong Yeon D Lee, San Ly, Jordi Garcia-Ojalvo, and Gürol M. Süel. Metabolic co-dependence gives rise to collective oscillations within biofilms. *Nature*, 523:550–554, 2015.

[25] Munehiro Asally, Mark Kittisopikul, Pau Rué, Yingjie Du, Zhenxing Hu, Tolga Çağatay, Andra B. Robinson, Hongbing Lu, Jordi Garcia-Ojalvo, and Gürol M. Süel. Localized cell death focuses mechanical forces during 3d patterning in a biofilm. *Proceedings of the National Academy of Sciences of the United States of America*, 109:18891–18896, 11 2012.

[26] Jintao Liu, Rosa Martinez-Corral, Arthur Prindle, Dong Yeon D. Lee, Joseph Larkin, Marçal Gabalda-Sagarra, Jordi Garcia-Ojalvo, and Gürol M. Süel. Coupling between distant biofilms and emergence of nutrient time-sharing. *Science*, 356:638–642, 2017.

[27] Katie Brenner, Lingchong You, and Frances H. Arnold. Engineering microbial consortia: a new frontier in synthetic biology. *Trends in Biotechnology*, 26:483–489, 2008.

[28] Kuili Fang, Oh Jin Park, and Seok Hoon Hong. Controlling biofilms using synthetic biology approaches. *Biotechnology Advances*, 40:107518, 2020.

[29] Thomas K. Wood, Seok Hoon Hong, and Qun Ma. Engineering biofilm formation and dispersal. *Trends in Biotechnology*, 29:87–94, 2 2011.

[30] Krystyna I. Wolska, Anna M. Grudniak, Zofia Rudnicka, and Katarzyna Markowska. Genetic control of bacterial biofilms. *Journal of Applied Genetics*, 57:225–238, 2016.

[31] Stephen J. Kassinger and Monique L. van Hoek. Biofilm architecture: An emerging synthetic biology target. *Synthetic and Systems Biotechnology*, 5:1–10, 2020.

[32] Sarah Guiziou, Vincent Sauveplane, Hung-Ju Chang, Caroline Clerté, Nathalie Declerck, Matthieu Jules, and Jerome Bonnet. A part toolbox to tune genetic expression in bacillus subtilis. *Nucleic acids research*, 44:7495–7508, 9 2016.

[33] Philipp F Popp, Mona Dotzler, Jara Radeck, Julia Bartels, and Thorsten Mascher. The bacillus biobrick box 2.0: expanding the genetic toolbox for the standardized work with bacillus subtilis. *Scientific Reports*, 7:15058, 2017.

[34] Sean P. Leonard, Jiri Perutka, J. Elijah Powell, Peng Geng, Darby D. Richhart, Michelle Byrom, Shaunak Kar, Bryan W. Davies, Andrew D. Ellington, Nancy A. Moran, and Jeffrey E. Barrick. Genetic engineering of bee gut microbiome bacteria with a toolkit for modular assembly of broad-host-range plasmids. *ACS Synthetic Biology*, 7:1279–1290, 2018.

[35] Christopher M. Thomas and Kaare M. Nielsen. Mechanisms of, and barriers to, horizontal gene transfer between bacteria. *Nature Reviews Microbiology*, 3:711–721, 2005.

[36] Gaoyan Wang, Zhiying Zhao, Jing Ke, Yvonne Engel, Yi-Ming Shi, David Robinson, Kerem Bingol, Zheyun Zhang, Benjamin Bowen, Katherine Louie, Bing Wang, Robert Evans, Yu Miyamoto, Kelly Cheng, Suzanne Kosina, Markus De Raad, Leslie Silva, Alicia Luhrs, Andrea Lubbe, David W Hoyt, Charles Francavilla, Hiroshi Otani, Samuel Deutsch, Nancy M Washton, Edward M Rubin, Nigel J Mouncey, Axel Visel, Trent Northen, Jan-Fang Cheng, Helge B Bode, and Yasuo Yoshikuni. Crage enables rapid activation of biosynthetic gene clusters in undomesticated bacteria. *Nature Microbiology*, 4:2498–2510, 2019.

[37] Carlotta Ronda, Sway P Chen, Vitor Cabral, Stephanie J Yaung, and Harris H Wang. Metagenomic engineering of the mammalian gut microbiome in situ. *Nature Methods*, 16:167–170, 2019.

[38] Jennifer A N Brophy, Alexander J Triassi, Bryn L Adams, Rebecca L Renberg, Dimitra N Stratis-Cullum, Alan D Grossman, and Christopher A Voigt. Engineered integrative and conjugative elements for efficient and inducible dna transfer to undomesticated bacteria. *Nature Microbiology*, 3:1043–1053, 2018.

[39] Xiaofan Jin and Ingmar H. Riedel-Kruse. Biofilm lithography enables high-resolution cell patterning via optogenetic adhesin expression. *Proceedings of the National Academy of Sciences of the United States of America*, 115:3698–3703, 2018.

[40] Chih-Yu Yang, Maja Bialecka-Fornal, Colleen Weatherwax, Joseph Larkin, Arthur Prindle, Jintao Liu, Jordi Garcia-Ojalvo, and Gurol M. Suel. Encoding spatial memory within a bacterial biofilm community. *Biophysical Journal*, 118:610a, 2020.

[41] Nicholas T. Ong, Evan J. Olson, and Jeffrey J. Tabor. Engineering an e. coli near-infrared light sensor. *ACS Synthetic Biology*, 7:240–248, 2018.

[42] Yajia Huang, Aiguo Xia, Guang Yang, and Fan Jin. Bioprinting living biofilms through optogenetic manipulation. *ACS Synthetic Biology*, 7:1195–1200, 5 2018. doi: 10.1021/acssynbio.8b00003.

[43] Sebastian M. Castillo-Hair, Elliot A. Baerman, Masaya Fujita, Oleg A. Igoshin, and Jeffrey J. Tabor. Optogenetic control of bacillus subtilis gene expression. *Nature Communications*, 10:1–11, 2019.

[44] Felix Moser, Eléonore Tham, Lina M. González, Timothy K. Lu, and Christopher A. Voigt. Light-controlled, high-resolution patterning of living engineered bacteria onto textiles, ceramics, and plastic. *Advanced Functional Materials*, 29:1–11, 2019.

[45] Nitai Steinberg and Ilana Kolodkin-Gal. The matrix reloaded: How sensing the extracellular matrix synchronizes bacterial communities. *Journal of Bacteriology*, 197:2092–2103, 2015.

[46] Hera Vlamakis, Yunrong Chai, Pascale Beauregard, Richard Losick, and Roberto Kolter. Sticking together: Building a biofilm the bacillus subtilis way. *Nature Reviews Microbiology*, 11:157–168, 2013.

[47] Peter Q. Nguyen, Zsofia Botyanszki, Pei Kun R. Tay, and Neel S. Joshi. Programmable biofilm-based materials from engineered curli nanofibres. *Nature Communications*, 5:1–10, 2014.

[48] Allen Y. Chen, Zhengtao Deng, Amanda N. Billings, Urartu O.S. Seker, Michelle Y. Lu, Robert J. Citorik, Bijan Zakeri, and Timothy K. Lu. Synthesis and patterning of tunable multiscale materials with engineered cells. *Nature Materials*, 13:515–523, 2014.

[49] Yangxiaolu Cao, Yaying Feng, Marc D. Ryser, Kui Zhu, Gregory Herschlag, Changyong Cao, Katherine Marusak, Stefan Zauscher, and Lingchong You. Programmable assembly of pressure sensors using pattern-forming bacteria. *Nature Biotechnology*, 35:1087–1093, 2017.

[50] Chen Zhang, Jiaofang Huang, Jicong Zhang, Suying Liu, Mengkui Cui, Bolin An, Xinyu Wang, Jiahua Pu, Tianxin Zhao, Chunhai Fan, Timothy K. Lu, and Chao Zhong. Engineered bacillus subtilis biofilms as living glues. *Materials Today*, 28:40–48, 9 2019.

[51] Jiaofang Huang, Suying Liu, Chen Zhang, Xinyu Wang, Jiahua Pu, Fang Ba, Shuai Xue, Haifeng Ye, Tianxin Zhao, Ke Li, Yanyi Wang, Jicong Zhang, Lihua Wang, Chunhai Fan, Timothy K. Lu, and Chao Zhong. Programmable and printable bacillus subtilis biofilms as engineered living materials. *Nature Chemical Biology*, 15:34–41, 2019.

[52] Jae Kyoung Kim, Ye Chen, Andrew J Hirning, Razan N Alnahhas, Krešimir Josić, and Matthew R Bennett. Long-range temporal coordination of gene expression in synthetic microbial consortia. *Nature Chemical Biology*, 15:1102–1109, 2019.

[53] Sonali Gupta, Tyler D. Ross, Marcella M. Gomez, Job L. Grant, Philip A. Romero, and Ophelia S. Venturelli. Investigating the dynamics of microbial consortia in spatially structured environments. *Nature Communications*, 11:1–15, 2020.

[54] Boyang Qin, Chenyi Fei, Andrew A. Bridges, Ameya A. Mashruwala, Howard A. Stone, Ned S. Wingreen, and Bonnie L. Bassler. Cell position fates and collective

fountain flow in bacterial biofilms revealed by light-sheet microscopy. *Science (New York, N.Y.)*, 369:71–77, 2020.

[55] Jacob T. Barlow, Said R. Bogatyrev, and Rustem F. Ismagilov. A quantitative sequencing framework for absolute abundance measurements of mucosal and lumenal microbial communities. *Nature Communications*, 11:1–13, 2020.

[56] Thomas M Norman, Nathan D Lord, Johan Paulsson, and Richard Losick. Memory and modularity in cell-fate decision making. *Nature*, 503:481–486, 2013.

[57] Declan A. Gray, Gaurav Dugar, Pamela Gamba, Henrik Strahl, Martijs J. Jonker, and Leendert W. Hamoen. Extreme slow growth as alternative strategy to survive deep starvation in bacteria. *Nature Communications*, 10:1–12, 2019.

[58] Jananee Jaishankar and Preeti Srivastava. Molecular basis of stationary phase survival and applications. *Frontiers in Microbiology*, 8:1–12, 2017.

[59] Orit Gefen, Ofer Fridman, Irine Ronin, and Nathalie Q. Balaban. Direct observation of single stationary-phase bacteria reveals a surprisingly long period of constant protein production activity. *Proceedings of the National Academy of Sciences of the United States of America*, 111:556–561, 2014.

[60] Arvi J oers and Tanel Tenson. Growth resumption from stationary phase reveals memory in escherichia coli cultures. *Scientific Reports*, 6:24055, 2016.

[61] C. Nicolella, M. C.M. Van Loosdrecht, and J. J. Heijnen. Wastewater treatment with particulate biofilm reactors. *Journal of Biotechnology*, 80:1–33, 2000.

[62] Bruce E. Logan. Exoelectrogenic bacteria that power microbial fuel cells. *Nature Reviews Microbiology*, 7:375–381, 2009.

[63] Kuili Fang, Xing Jin, and Seok Hoon Hong. Probiotic escherichia coli inhibits biofilm formation of pathogenic e. coli via extracellular activity of degp. *Scientific Reports*, 8:4939, 2018.

[64] Anna M. Duraj-Thatte, Pichet Praveschotinunt, Trevor R. Nash, Frederick R. Ward, and Neel S. Joshi. Modulating bacterial and gut mucosal interactions with engineered biofilm matrix proteins. *Scientific Reports*, 8:1–8, 2018.

[65] Xinyue Wang, Zhenping Cao, Mengmeng Zhang, Lu Meng, Zunzhen Ming, and Jinyao Liu. Bioinspired oral delivery of gut microbiota by self-coating with biofilms. *Science Advances*, 6, 2020.

[66] Michael P. O'Donnell, Bennett W. Fox, Pin Hao Chao, Frank C. Schroeder, and Piali Sengupta. A neurotransmitter produced by gut bacteria modulates host sensory behaviour. *Nature*, 583:415–420, 2020.

[67] Pei Kun R. Tay, Avinash Manjula-Basavanna, and Neel S. Joshi. Repurposing bacterial extracellular matrix for selective and differential abstraction of rare earth elements. *Green Chemistry*, 20:3512–3520, 2018.

[68] Pei Kun R. Tay, Peter Q. Nguyen, and Neel S. Joshi. A synthetic circuit for mercury bioremediation using self-assembling functional amyloids. *ACS Synthetic Biology*, 6:1841–1850, 2017.

[69] David T. Riglar, Tobias W. Giessen, Michael Baym, S. Jordan Kerns, Matthew J. Niederhuber, Roderick T. Bronson, Jonathan W. Kotula, Georg K. Gerber, Jeffrey C. Way, and Pamela A. Silver. Engineered bacteria can function in the mammalian gut long-term as live diagnostics of inflammation. *Nature Biotechnology*, 35:653–658, 2017.

[70] Ilaria Benedetti, Víctor de Lorenzo, and Pablo I. Nikel. Genetic programming of catalytic pseudomonas putida biofilms for boosting biodegradation of haloalkanes. *Metabolic Engineering*, 33:109–118, 2016.

[71] Manisha Mukherjee, Yidan Hu, Chuan Hao Tan, Scott A. Rice, and Bin Cao. Engineering a light-responsive, quorum quenching biofilm to mitigate biofouling on water purification membranes. *Science Advances*, 4, 2018.

[72] Nicole M Vega and Jeff Gore. Collective antibiotic resistance: mechanisms and implications. *Current Opinion in Microbiology*, 21:28–34, 2014.

[73] Hannah R Meredith, Jaydeep K Srimani, Anna J Lee, Allison J Lopatkin, and Lingchong You. Collective antibiotic tolerance: mechanisms, dynamics and intervention. *Nature Chemical Biology*, 11:182, 2015.

[74] Ophelia S Venturelli, Alex V Carr, Garth Fisher, Ryan H Hsu, Rebecca Lau, Benjamin P Bowen, Susan Hromada, Trent Northen, and Adam P Arkin. Deciphering microbial interactions in synthetic human gut microbiome communities. *Molecular Systems Biology*, 14:1–19, 2018.

[75] Wentao Kong, David R Meldgin, James J Collins, and Ting Lu. Designing microbial consortia with defined social interactions. *Nature Chemical Biology*, 14:821–829, 2018.

[76] J C Ray, J J Tabor, and O A Igoshin. Non-transcriptional regulatory processes shape transcriptional network dynamics. *Nat Rev Microbiol*, 9:817–828, 2011.

[77] Jonathan Friedman, Logan M Higgins, and Jeff Gore. Community structure follows simple assembly rules in microbial microcosms. *Nature Ecology I&Amp; Evolution*, 1:109, 2017.

[78] Michael T Mee, James J Collins, George M Church, and Harris H Wang. Syntrophic exchange in synthetic microbial communities. *Proceedings of the National Academy of Sciences*, 111:E2149, 2014.

[79] P S Stewart and M J Franklin. Physiological heterogeneity in biofilms. *Nat Rev Microbiol*, 6:199–210, 2008.

[80] Philip S Stewart and J William Costerton. Antibiotic resistance of bacteria in biofilms. *The Lancet*, 358:135–138, 2001.

[81] Ting Lu, Tongye Shen, Matthew R Bennett, Peter G Wolynes, and Jeff Hasty. Phenotypic variability of growing cellular populations. *Proceedings of the National Academy of Sciences*, 104:18982, 2007.

[82] James A Damore and Jeff Gore. Understanding microbial cooperation. *Journal of Theoretical Biology*, 299:31–41, 2012.

[83] Eshel Ben-Jacob, Inon Cohen, and Herbert Levine. Cooperative self-organization of microorganisms. *Advances in Physics*, 49:395–554, 2000.

[84] Michael A Lobritz, Peter Belenky, Caroline B M Porter, Arnaud Gutierrez, Jason H Yang, Eric G Schwarz, Daniel J Dwyer, Ahmad S Khalil, and James J Collins. Antibiotic efficacy is linked to bacterial cellular respiration. *Proceedings of the National Academy of Sciences*, 112:8173 LP – 8180, 7 2015.

[85] D J Dwyer, P A Belenky, J H Yang, I C MacDonald, J D Martell, N Takahashi, C T Chan, M A Lobritz, D Braff, E G Schwarz, J D Ye, M Pati, M Vercruysse, P S Ralifo, K R Allison, A S Khalil, A Y Ting, G C Walker, and J J Collins. Antibiotics induce redox-related physiological alterations as part of their lethality. *Proc Natl Acad Sci U S A*, 111:E2100–9, 2014.

[86] Tiebin Wang, Imane El Meouche, and Mary J Dunlop. Bacterial persistence induced by salicylate via reactive oxygen species. *Scientific Reports*, 7:43839, 2017.

[87] Imane El Meouche, Yik Siu, and Mary J Dunlop. Stochastic expression of a multiple antibiotic resistance activator confers transient resistance in single cells. *Scientific Reports*, 6:19538, 2016.

[88] David Davies. Understanding biofilm resistance to antibacterial agents. *Nature Reviews Drug Discovery*, 2:114, 2003.

[89] Sashi Nadanaciva, Payal Rana, Gyda C Beeson, Denise Chen, David A Ferrick, Craig C Beeson, and Yvonne Will. Assessment of drug-induced mitochondrial dysfunction via altered cellular respiration and acidification measured in a 96-well platform. *Journal of Bioenergetics and Biomembranes*, 44:421–437, 2012.

[90] Christopher G R Perry, Daniel A Kane, Ian R Lanza, and P Darrell Neufer. Methods for assessing mitochondrial function in diabetes. *Diabetes*, 62:1041 LP – 1053, 4 2013.

[91] Ajit S Divakaruni, Alexander Paradyse, David A Ferrick, Anne N Murphy, and Martin Jastroch. Chapter sixteen - analysis and interpretation of microplate-based oxygen consumption and ph data. *Mitochondrial Function*, 547:309–354, 2014.

[92] Daniel B Kearns, Frances Chu, Steven S Branda, Roberto Kolter, and Richard Losick. A master regulator for biofilm formation by bacillus subtilis. *Molecular Microbiology*, 55:739–749, 2004.

[93] Daniel J Dwyer, Michael A Kohanski, Boris Hayete, and James J Collins. Gyrase inhibitors induce an oxidative damage cellular death pathway in escherichia coli. *Molecular Systems Biology*, 3:91, 2007.

[94] Michael A Kohanski, Daniel J Dwyer, Boris Hayete, Carolyn A Lawrence, and James J Collins. A common mechanism of cellular death induced by bactericidal antibiotics. *Cell*, 130:797–810, 2007.

[95] Elena B M Breidenstein, Bhavjinder K Khaira, Irith Wiegand, Joerg Overhage, and Robert E W Hancock. Complex ciprofloxacin resistome revealed by screening

a pseudomonas aeruginosa mutant library for altered susceptibility. *Antimicrobial agents and chemotherapy*, 52:4486–4491, 2008.

[96] Bryan W Davies, Michael A Kohanski, Lyle A Simmons, Jonathan A Winkler, James J Collins, and Graham C Walker. Hydroxyurea induces hydroxyl radical-mediated cell death in escherichia coli. *Molecular Cell*, 36:845–860, 2009.

[97] Xiuhong Wang and Xilin Zhao. Contribution of oxidative damage to antimicrobial lethality. *Antimicrobial agents and chemotherapy*, 53:1395, 2009.

[98] H Kanafani and S E Martin. Catalase and superoxide dismutase activities in virulent and nonvirulent staphylococcus aureus isolates. *Journal of clinical microbiology*, 21:607–610, 1985.

[99] Vinai C Thomas, Lauren C Kinkead, Ashley Janssen, Carolyn R Schaeffer, Keith M Woods, Jill K Lindgren, Jonathan M Peaster, Sujata S Chaudhari, Marat Sadykov, Joselyn Jones, Sameh M Mohamadi AbdelGhani, Matthew C Zimmerman, Kenneth W Bayles, Greg A Somerville, and Paul D Fey. A dysfunctional tricarboxylic acid cycle enhances fitness of staphylococcus epidermidis during $\beta$-lactam stress. *mBio*, 4:e00437–13, 2013.

[100] Terry A Krulwich, George Sachs, and Etana Padan. Molecular aspects of bacterial ph sensing and homeostasis. *Nature Reviews Microbiology*, 9:330–343, 2011.

[101] Keith A. Martinez, Ryan D. Kitko, J. Patrick Mershon, Haley E. Adcox, Kotiba A. Malek, Melanie B. Berkmen, and Joan L. Slonczewski. Cytoplasmic ph response

to acid stress in individual cells of escherichia coli and bacillus subtilis observed by fluorescence ratio imaging microscopy. *Applied and Environmental Microbiology*, 78:3706–3714, 2012.

[102] Michel Fasnacht and Norbert Polacek. Oxidative stress in bacteria and the central dogma of molecular biology. *Frontiers in Molecular Biosciences*, 8, 2021.

[103] K R Allison, M P Brynildsen, and J J Collins. Metabolite-enabled eradication of bacterial persisters by aminoglycosides. *Nature*, 473:216–220, 2011.

[104] Matthew G Vander Heiden, Lewis C Cantley, and Craig B Thompson. Understanding the warburg effect: the metabolic requirements of cell proliferation. *Science (New York, N.Y.)*, 324:1029–1033, 2009.

[105] Sean C Booth, Matthew L Workentine, Jing Wen, Rustem Shaykhutdinov, Hans J Vogel, Howard Ceri, Raymond J Turner, and Aalim M Weljie. Differences in metabolism between the biofilm and planktonic response to metal stress. *Journal of Proteome Research*, 10:3190–3199, 2011.

[106] Ilana Kolodkin-Gal, Alexander K W Elsholz, Christine Muth, Peter R Girguis, Roberto Kolter, and Richard Losick. Respiration control of multicellularity in bacillus subtilis by a complex of the cytochrome chain with a membrane-embedded histidine kinase. *Genes & development*, 27:887–899, 2013.

[107] Lars E P Dietrich, Chinweike Okegbe, Alexa Price-Whelan, Hassan Sakhtah, Ryan C Hunter, and Dianne K Newman. Bacterial community morphogenesis is

intimately linked to the intracellular redox state. *Journal of Bacteriology*, 195:1371, 2013.

[108] Markus Basan, Sheng Hui, Hiroyuki Okano, Zhongge Zhang, Yang Shen, James R Williamson, and Terence Hwa. Overflow metabolism in escherichia coli results from efficient proteome allocation. *Nature*, 528:99–104, 2015.

[109] Wolfe Alan J. The acetate switch. *Microbiology and Molecular Biology Reviews*, 69:12–50, 3 2005. doi: 10.1128/MMBR.69.1.12-50.2005.

[110] Jorge Fernandez de Cossio-Diaz and Alexei Vazquez. Limits of aerobic metabolism in cancer cells. *Scientific reports*, 7:13488, 10 2017.

[111] Irvin N Hirshfield, Stephanie Terzulli, and Conor O'Byrne. Weak organic acids: A panoply of effects on bacteria. *Science Progress*, 86:245–270, 11 2003. doi: 10.3184/003685003783238626.

[112] James B Russell and Francisco Diez-Gonzalez. The effects of fermentation acids on bacterial growth. In R K B T Advances in Microbial Physiology Poole, editor, *Adv Microb Physiol*, volume 39, pages 205–234. Academic Press, 1997.

[113] Laura Preiss, David B Hicks, Shino Suzuki, Thomas Meier, and Terry Ann Krulwich. Alkaliphilic bacteria with impact on industrial applications, concepts of early life forms, and bioenergetics of atp synthesis. *Frontiers in Bioengineering and Biotechnology*, 3:75, 2015.

[114] Wilfred J Ferguson, K I Braunschweiger, W R Braunschweiger, James R Smith, J.Justin McCormick, Cathy C Wasmann, Nancy P Jarvis, Duncan H Bell, and Norman E Good. Hydrogen ion buffers for biological research. *Analytical Biochemistry*, 104:300–310, 1980.

[115] Norman E Good, G Douglas Winget, Wilhelmina Winter, Thomas N Connolly, Seikichi Izawa, and Raizada M M Singh. Hydrogen ion buffers for biological research*. *Biochemistry*, 5:467–477, 2 1966. doi: 10.1021/bi00866a011.

[116] Gustavo A Ramírez, Arkadiy I Garber, Aurélien Lecoeuvre, Timothy D'Angelo, C Geoffrey Wheat, and Beth N Orcutt. Ecology of subseafloor crustal biofilms. *Frontiers in Microbiology*, 10:1983, 2019.

[117] Bart Hens, Yasuhiro Tsume, Marival Bermejo, Paulo Paixao, Mark J Koenigsknecht, Jason R Baker, William L Hasler, Robert Lionberger, Jianghong Fan, Joseph Dickens, Kerby Shedden, Bo Wen, Jeffrey Wysocki, Raimar Loebenberg, Allen Lee, Ann Frances, Greg Amidon, Alex Yu, Gail Benninghoff, Niloufar Salehi, Arjang Talattof, Duxin Sun, and Gordon L Amidon. Low buffer capacity and alternating motility along the human gastrointestinal tract: Implications for in vivo dissolution and absorption of ionizable drugs. *Molecular Pharmaceutics*, 14:4281–4294, 12 2017. doi: 10.1021/acs.molpharmaceut.7b00426.

[118] David Fernández-Calvi no and Erland Bååth. Growth response of the bacterial community to ph in soils differing in ph. *FEMS Microbiology Ecology*, 73:149–156, 7 2010.

[119] Wei-Jun Cai, Wei-Jen Huang, George W Luther, Denis Pierrot, Ming Li, Jeremy Testa, Ming Xue, Andrew Joesoef, Roger Mann, Jean Brodeur, Yuan-Yuan Xu, Baoshan Chen, Najid Hussain, George G Waldbusser, Jeffrey Cornwell, and W Michael Kemp. Redox reactions and weak buffering capacity lead to acidification in the chesapeake bay. *Nature Communications*, 8:369, 2017.

[120] Yuting Zhang, Hong Shen, Xinhua He, Ben W Thomas, Newton Z Lupwayi, Xiying Hao, Matthew C Thomas, and Xiaojun Shi. Fertilization shapes bacterial community structure by alteration of soil ph. *Frontiers in Microbiology*, 8, 2017.

[121] M Kihara and R M Macnab. Cytoplasmic ph mediates ph taxis and weak-acid repellent taxis of bacteria. *Journal of Bacteriology*, 145:1209–1221, 1981.

[122] Tohidifar Payman, Plutz Matthew J, Ordal George W, and Rao Christopher V. The mechanism of bidirectional ph taxis in bacillus subtilis. *Journal of Bacteriology*, 202:e00491–19, 1 2020. doi: 10.1128/JB.00491-19.

[123] Jagadish Sankaran, Nicholas J H J Tan, Ka Pui But, Yehuda Cohen, Scott A Rice, and Thorsten Wohland. Single microcolony diffusion analysis in pseudomonas aeruginosa biofilms. *npj Biofilms and Microbiomes*, 5:35, 2019.

[124] Philip S Stewart. Diffusion in biofilms. *Journal of Bacteriology*, 185:1485–1491, 2003.

[125] Paula Watnick and Roberto Kolter. Biofilm, city of microbes. *Journal of Bacteriology*, 182:2675–2679, 5 2000.

[126] Hugo Cruz Ramos, Tamara Hoffmann, Marco Marino, Hafed Nedjari, Elena Presecan-Siedel, Oliver Dreesen, Philippe Glaser, and Dieter Jahn. Fermentative metabolism of bacillus subtilis: Physiology and regulation of gene expression. *Journal of Bacteriology*, 182:3072–3080, 2000.

[127] Rob Van Houdt, Abram Aertsen, and Chris W Michiels. Quorum-sensing-dependent switch to butanediol fermentation prevents lethal medium acidification in aeromonas hydrophila ah-1n. *Research in Microbiology*, 158:379–385, 2007.

[128] Bram Vivijs, Pieter Moons, Abram Aertsen, and Chris W Michiels. Acetoin synthesis acquisition favors escherichia coli growth at low ph. *Applied and environmental microbiology*, 80:6054–6061, 10 2014.

[129] Katrine L Whiteson, Simone Meinardi, Yan Wei Lim, Robert Schmieder, Heather Maughan, Robert Quinn, Donald R Blake, Douglas Conrad, and Forest Rohwer. Breath gas metabolites and bacterial metagenomes from cystic fibrosis airways indicate active ph neutral 2,3-butanedione fermentation. *The ISME Journal*, 8:1247–1258, 2014.

[130] Elliott P. Barnhart, Marcella A. McClure, Kiki Johnson, Sean Cleveland, Kristopher A. Hunt, and Matthew W. Fields. Potential role of acetyl-coa synthetase (acs) and malate dehydrogenase (mae) in the evolution of the acetate switch in bacteria and archaea. *Scientific Reports*, 5:1–10, 2015.

[131] Bradley G Lusk, Isaias Peraza, Gaurav Albal, Andrew K Marcus, Sudeep C Popat, and Cesar I Torres. ph dependency in anode biofilms of thermincola ferriacetica suggests a proton-dependent electrochemical response. *Journal of the American Chemical Society*, 140:5527–5534, 4 2018. doi: 10.1021/jacs.8b01734.

[132] Sara Tejedor-Sanz, Eric T Stevens, Siliang Li, Peter Finnegan, James Nelson, Andre Knoesen, Samuel H Light, Caroline M Ajo-Franklin, and Maria L Marco. Extracellular electron transfer increases fermentation in lactic acid bacteria via a hybrid metabolism. *eLife*, 11:e70684, 2022.

[133] Andrés Aranda-Díaz, Benjamin Obadia, Ren Dodge, Tani Thomsen, Zachary F Hallberg, Zehra Tüzün Güvener, William B Ludington, and Kerwyn Casey Huang. Bacterial interspecies interactions modulate ph-mediated antibiotic tolerance. *eLife*, 9:e51493, 2020.

[134] Robert Mugabi, Daniel Sandgren, Ms Megan Born, Ian Leith, Shelley M Horne, and Birgit M Prüß. The role of activated acetate intermediates in the control of escherichia coli biofilm amounts. *WebmedCentral*, 3, 2012.

[135] Alan J. Wolfe, Dong Eun Chang, Jason D. Walker, Jeanine E. Seitz-Partridge, Michael D. Vidaurri, Charles F. Lange, Birgit M. Prüß, Margaret C. Henk, John C. Larkin, and Tyrrell Conway. Evidence that acetyl phosphate functions as a global signal during biofilm development. *Molecular Microbiology*, 48:977–988, 2003.

[136] Melissa A. Konkol, Kris M. Blair, and Daniel B. Kearns. Plasmid-encoded comi inhibits competence in the ancestral 3610 strain of bacillus subtilis. *Journal of Bacteriology*, 195:4085–4093, 2013.

APPENDIX A

# Appendix 1

## A.1. Scientific illustration

During my time at Northwestern University, I have become deeply interested in both the illustration and communication of scientific concepts and data. Towards this, I have created various figures for events, successfully funded grants and publications. This would not be at all possible without the excellent feedback from my lab mates, advisors, and collaborators. All illustrations were created in Adobe Photoshop and Illustrator.


**Figure A.1.** Logo for the inaugural Central US Synthetic Biology Workshop in 2018. This logo is now used as the basis for all workshops since 2018.

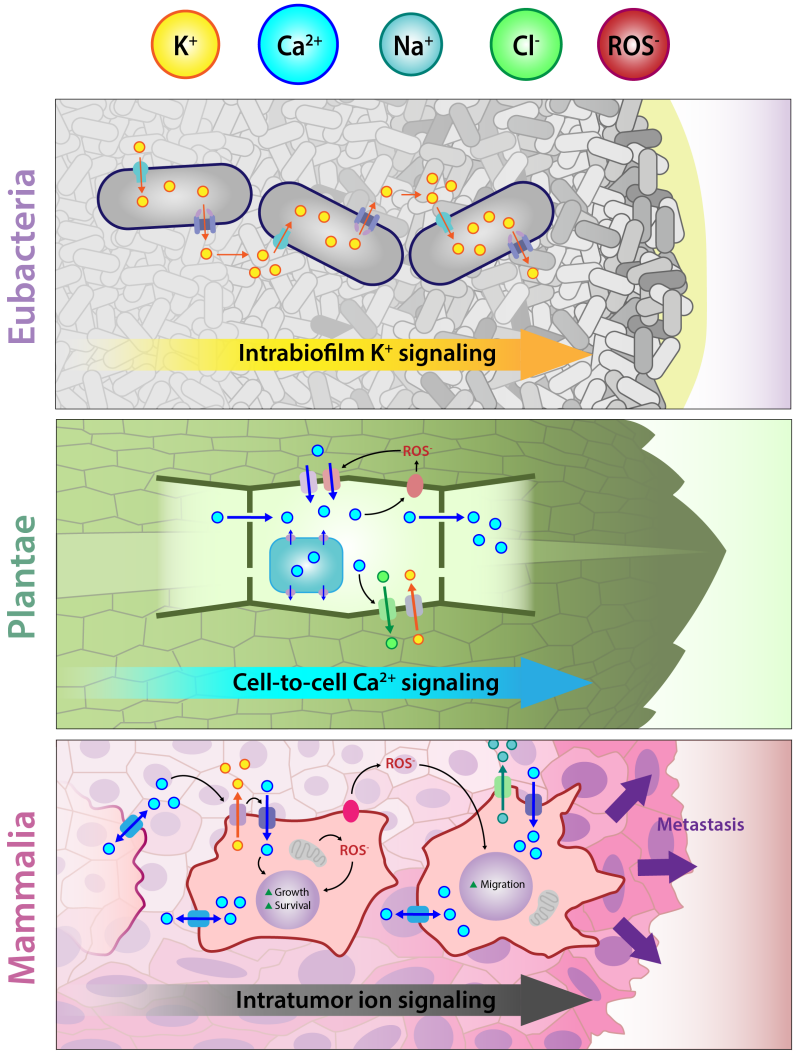


**Figure A.2.** Recent research shows that both prokaryotes and eukaryotes use ion- and redox-based electrochemical signals for communication. It has been shown thatsuch communication enables the organization of growth and developmental processes across multiple length scales. This figure was used in Schofield *et al*, J R Soc Interface, 2020.

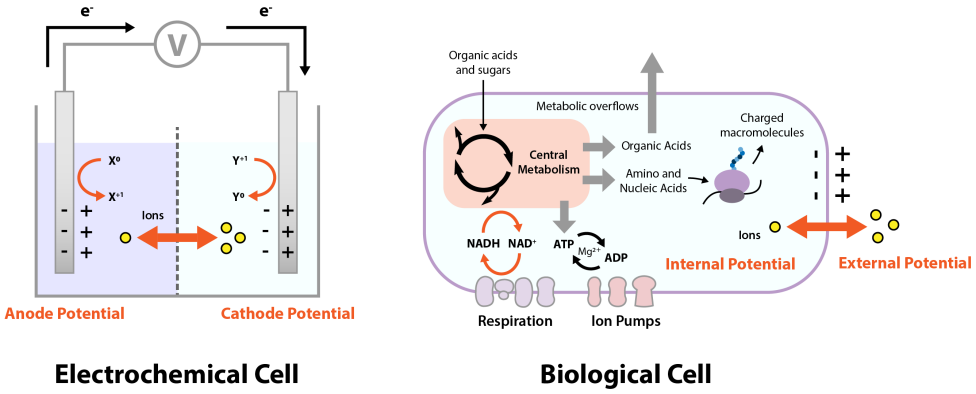


**Figure A.3.** The basis for a bioelectrical view of cells can be motivated by drawing an analogy between a battery (a) and a biological cell (b). Both systems rely on ionflows and redox reactions across interfaces. This figure was used in Schofield *et al*, J R Soc Interface, 2020.

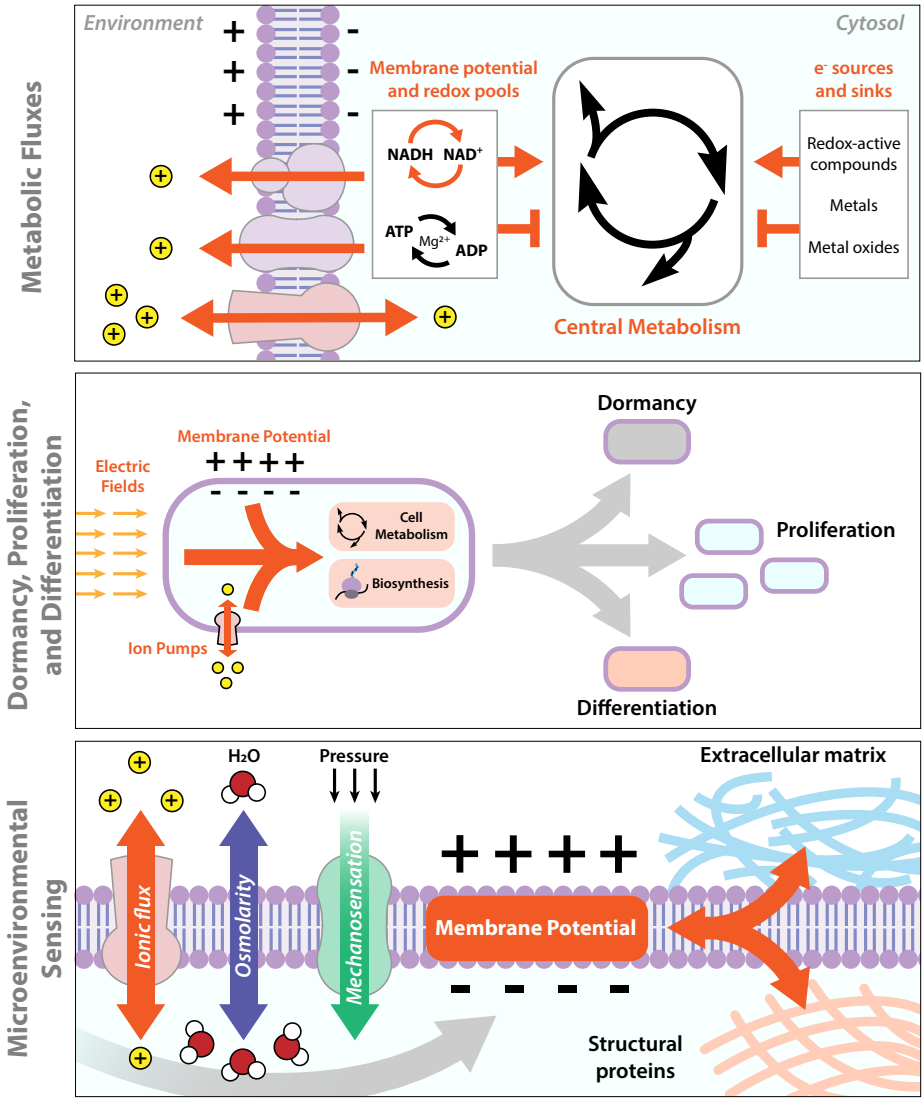


**Figure A.4.** Cartoon illustration of the coupling between the bioelectrical nature of the cell, in particular MP and IMF, and higher level cellular behaviours. This figure was used in Schofield *et al*, J R Soc Interface, 2020.

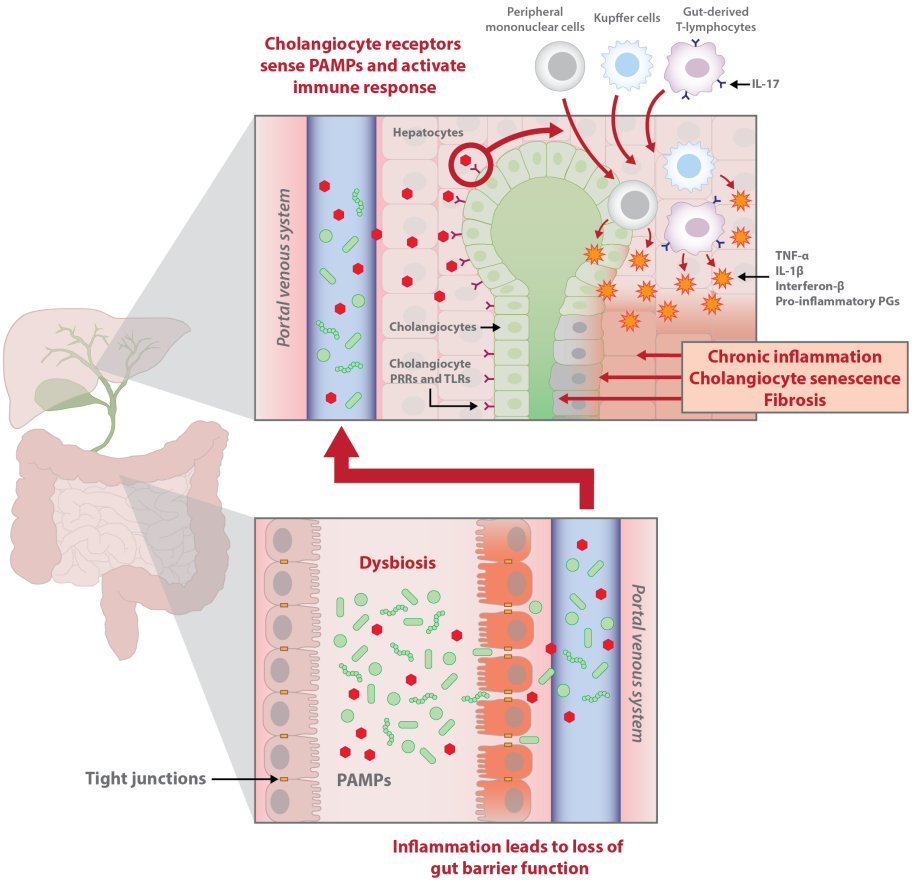


**Figure A.5.** PSC patients exhibit decreased enteric microbial diversity and altered species abundances (dysbiosis). These bacteria are thought to produce toxins, or PAMPs, which, in the setting of mucosal inflammation, translocate paracellularly into the portal venous system and travel to the liver. Here they are thought to stimulate an immune response, mediated by hepatic and peripheral lymphocytes as well as gut-derived T-lymphocytes which are activated by intestinal antigens. When chronic, this process leads to cholangiocyte senescence and fibrosis. Abbreviations: IL, interleukin; PAMP, pathogen-associated molecular protein; PG, prostaglandin; PRR, pattern recognition receptor; TLR, toll-like receptor; TNF-$\alpha$, tumor necrosis factor-alpha. This figure was used in Dean *et al*, Hepatology, 2020 and appeared on the cover of Hepatology Vol. 72, Sept. 2020

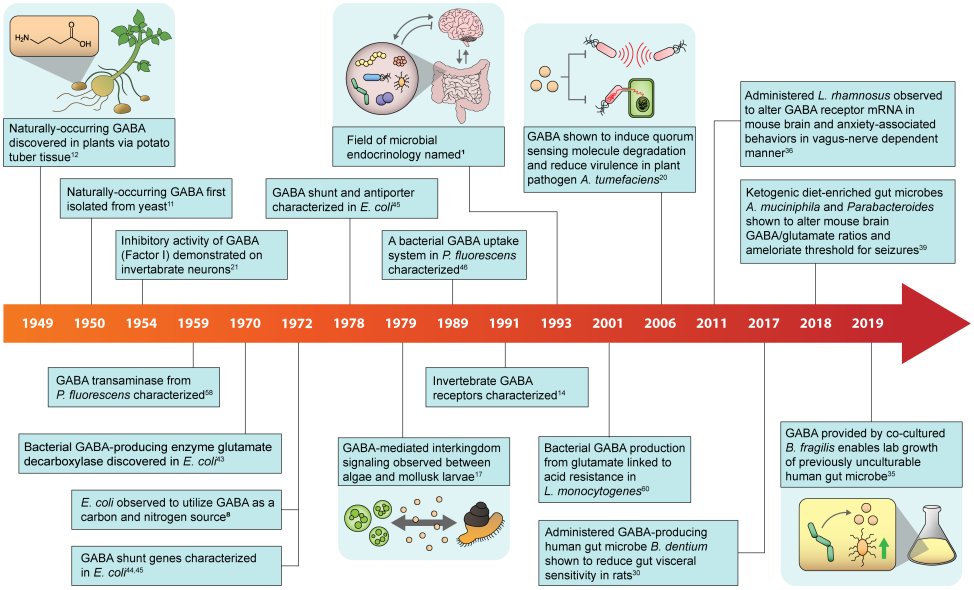


**Figure A.6.** A timeline depicting major discoveries relating to the potential for GABA as an interkingdom signaling moleculeand as a signaling molecule within bacterial communities. GABA, gamma-aminobutyric acid. This figure was used in Quillin *et al*, Bioelectricity, 2021.

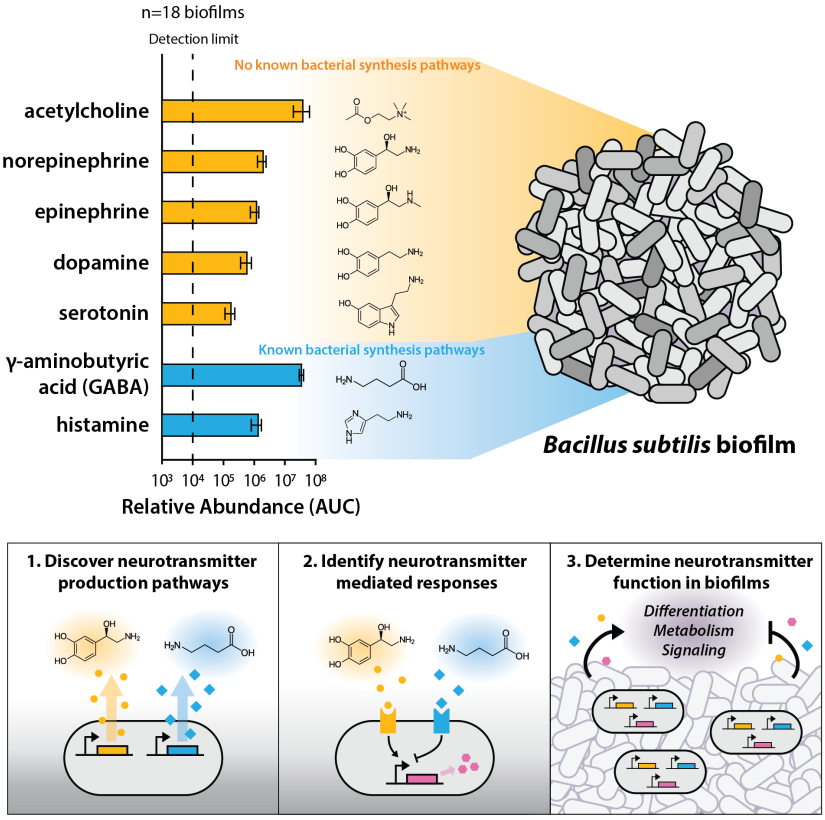


**Figure A.7.** Discovery of endogenously produced neurotransmitters in *B. subtilis* biofilms and proposed research plan. This figure was used in a successfully funded ECASE 2021 application.

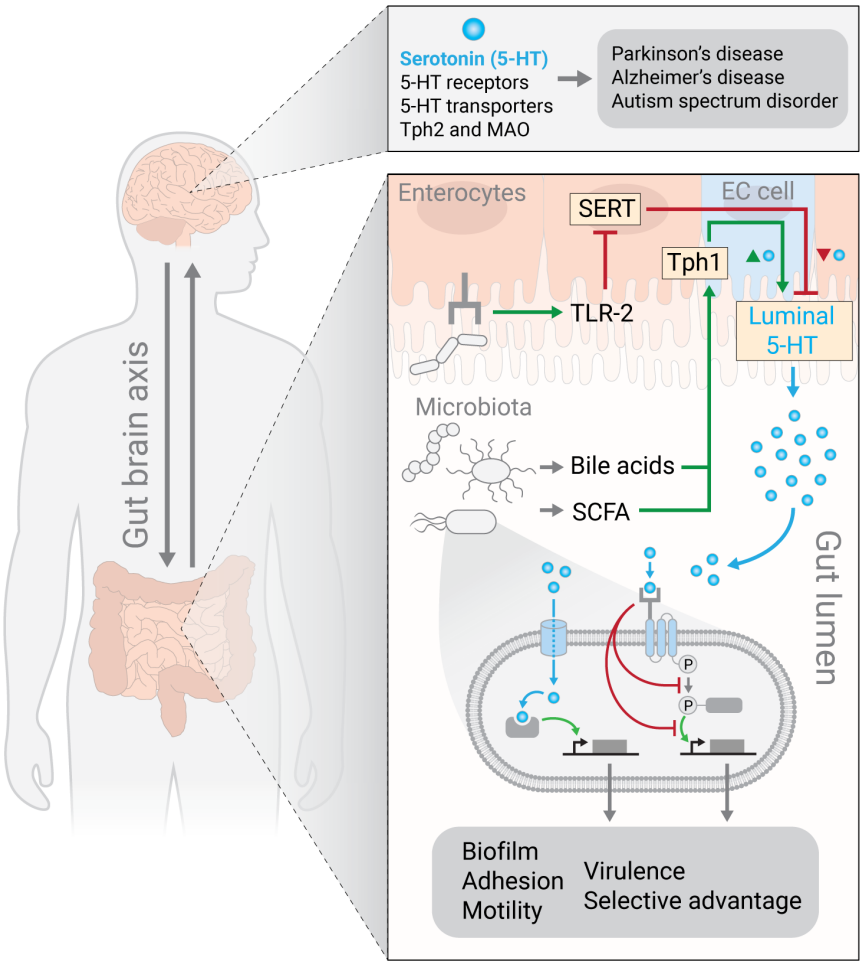


**Figure A.8.** Serotonin signaling occurs bidirectionally between the host and members of the microbiome and may contribute to disease. Bacteria residing in the gut lumen can sense serotonin levels that can induce and/or inhibit gene expression related to biofilm formation, adhesion, motility, or virulence. The levels of luminal serotonin can also provide a selective advantage for certain species. Some microbiota can also increase luminal serotonin concentrations via increased expression of serotonin-synthesis enzymes, such as TpH1, or decreased expression of the SERT, and potentially other undefined mechanisms. These effects can be mediated by secreted bacterial secondary metabolites, or via interaction between the microbes and host receptors. Further, due to the existence of the gut-brain axis, microbiota can influence the levels of brain serotonin levels by modulating expression of serotonin, receptors, transporters, and synthesis, and metabolic enzymes, such as TpH2 and MAO. It is hypothesized that these microbiota-mediated changes in serotonin contribute to multiple neurological conditions. This figure was used in Everett *et al*, Curr Opin Biotechnol, 2022.

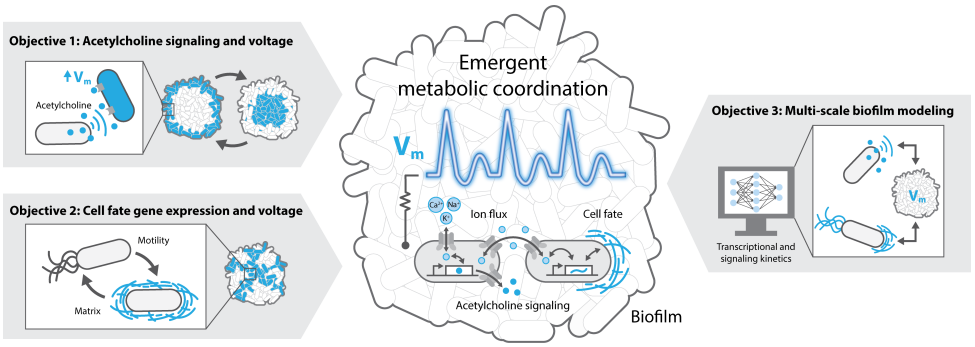


**Figure A.9.** Proposed research plan for deciphering the fundamental molecular mechanisms underlying metabolic coordination and cell-to-cell signaling in bacterial biofilms. This figure was used in a successfully funded NSF Career 2022 application.